# *The “magic” barrier before thermalization*

## and other topics

*Berndt Mueller* (Duke Univ.)

Wigner Institute

26 February 2026

Budapest, Hungary

# The Team

- Vincent Chen (Duke University - undergrad. student)
- Lukas Ebner (LMU München, Ph.D. student)
- Andreas Schäfer (Regensburg, Professor emeritus)
- Leonhard Schmotzer (Regensburg, masters student)
- Clemens Seidl (Regensburg, Ph.D. student)
- Xiaojun Yao (IQuS Seattle, assistant professor)
- BM

- Main articles/preprints:
  - *Commun. Phys.* 8 (2025) 368 [2411.04550]
  - 2510.11681 [quant-ph]
  - 2601.10065 [hep-lat]

# Overview

- Motivation
- Hamiltonian Lattice Gauge Theory
- Spectral form factor and energy diffusion
- Two-step thermalization
- The “Magic Barrier”
- SU(3) lattice gauge theory
  - Minimal truncation scheme
  - Quantum chaotic properties
  - $Q\bar{Q}$ and $QQQ$ potential

# (2+1)-D SU(2) Lattice Gauge Theory

Kogut-Susskind Hamiltonian: $$H = \frac{g^2}{2}\sum_{\text{links}}(E_i^a)^2 - \frac{2}{a^2g^2}\sum_{\text{plaquettes}}\Box(\boldsymbol{n})$$

$$\Box(\boldsymbol{n}) = \mathrm{Tr}[U^\dagger(\boldsymbol{n},\hat{y})U^\dagger(\boldsymbol{n}+\hat{y},\hat{x})U(\boldsymbol{n}+\hat{x},\hat{y})U(\boldsymbol{n},\hat{x})]$$

$$[E_i^a, U(\boldsymbol{n},\hat{j})] = -\delta_{ij}T^aU(\boldsymbol{n},\hat{j})$$

$$[E_i^a, E_i^b] = if^{abc}E_i^c$$

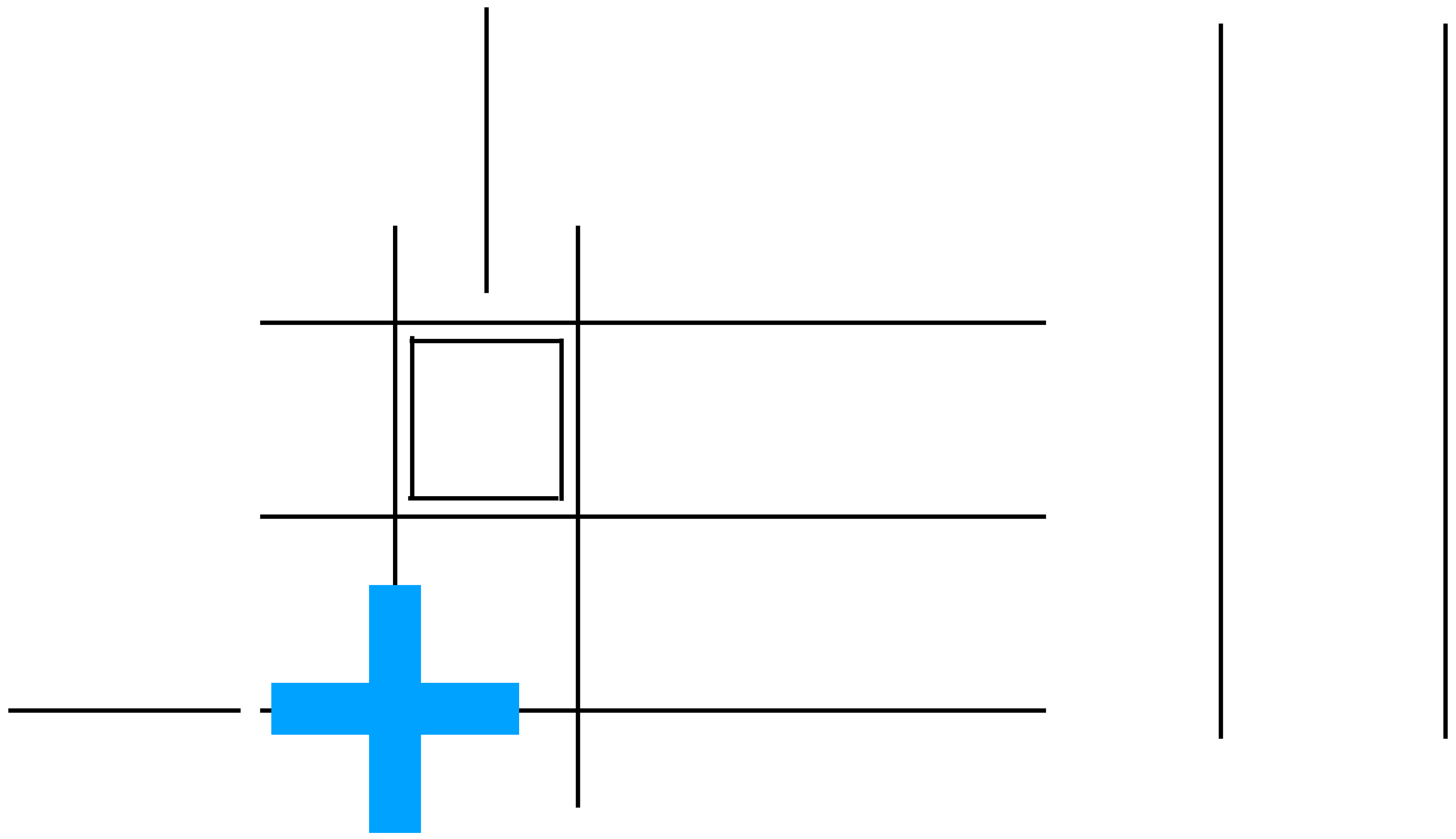

Gauss's law: Every vertex transforms as a singlet for a state to be physical

Electric basis on links: $|j\,m_L\,m_R\rangle$

$$E^2|j\,m_L\,m_R\rangle = j(j+1)|j\,m_L\,m_R\rangle$$

Byrnes, Yamamoto, quant-ph/0510027

# (2+1)-D SU(2) on Periodic Plaquette Chain

Each vertex has three links: singlet is uniquely defined by the $j$ values on the three links

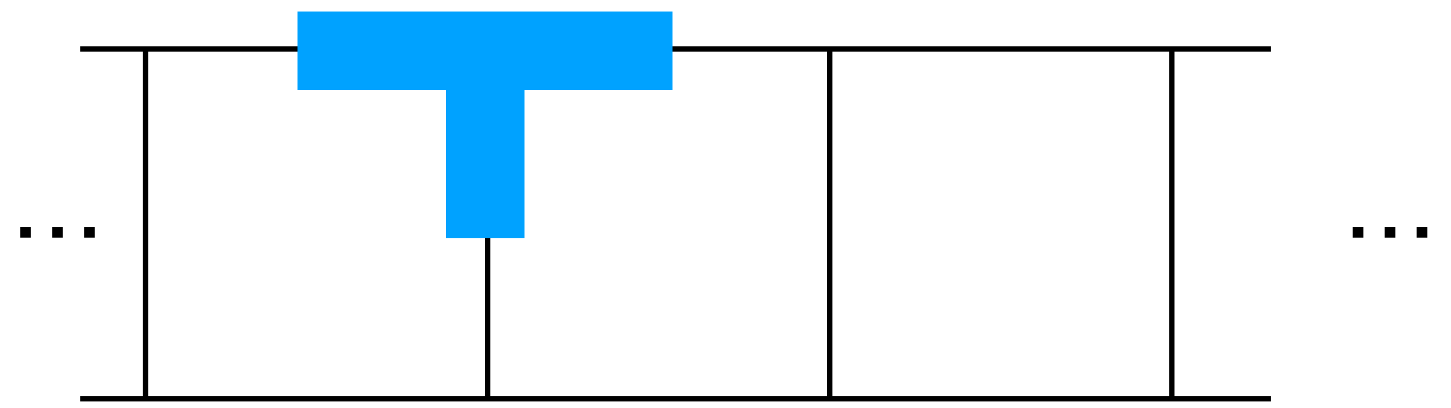


Klco, Stryker, Savage, 1908.06935

Matrix elements between physical states (singlets) expressed in 6$j$ symbols

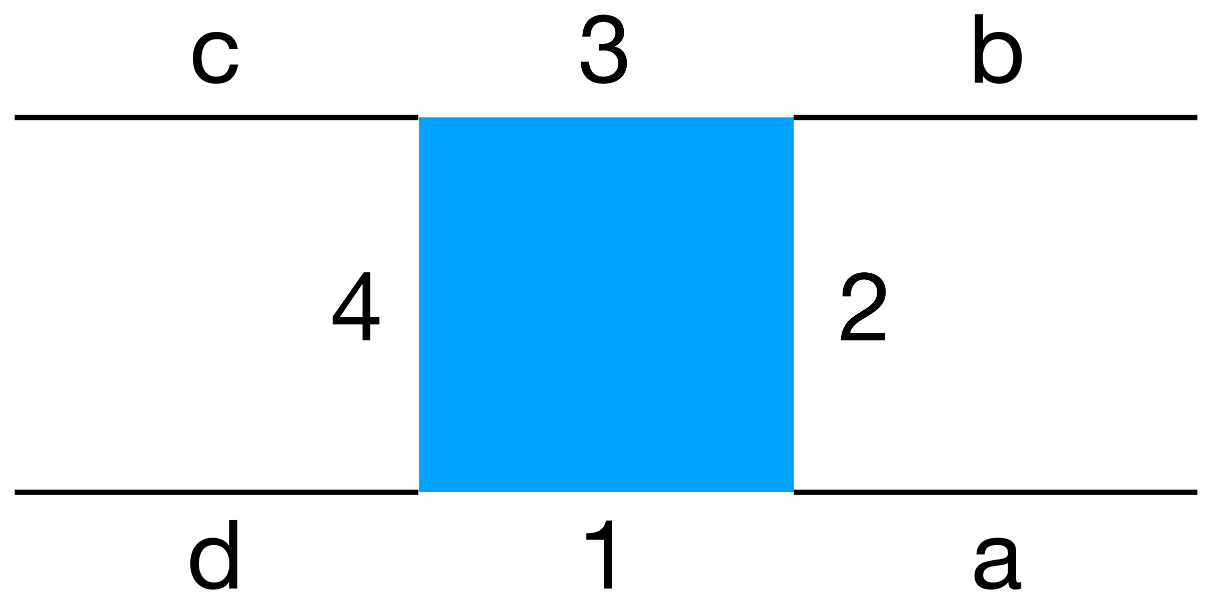


$j$: initial

$J$: final

$$\langle J_1 J_2 J_3 J_4 | \Box | j_1 j_2 j_3 j_4 \rangle = \prod_{\alpha=a,b,c,d} (-1)^{j_\alpha} \prod_{\alpha=1,2,3,4} \left[ (-1)^{j_\alpha + J_\alpha} \sqrt{(2j_\alpha+1)(2J_\alpha+1)} \right]$$

$$\begin{Bmatrix} j_a & j_1 & j_2 \\ 1/2 & J_2 & J_1 \end{Bmatrix} \begin{Bmatrix} j_b & j_2 & j_3 \\ 1/2 & J_3 & J_2 \end{Bmatrix} \begin{Bmatrix} j_c & j_3 & j_4 \\ 1/2 & J_4 & J_3 \end{Bmatrix} \begin{Bmatrix} j_d & j_4 & j_1 \\ 1/2 & J_1 & J_4 \end{Bmatrix}$$

Also for honeycomb lattice (2307.00045)

# (2+1)-D SU(2) on Honeycomb Lattice

On square lattice each vertex has four links and singlet is not unique

Solution: use honeycomb lattice

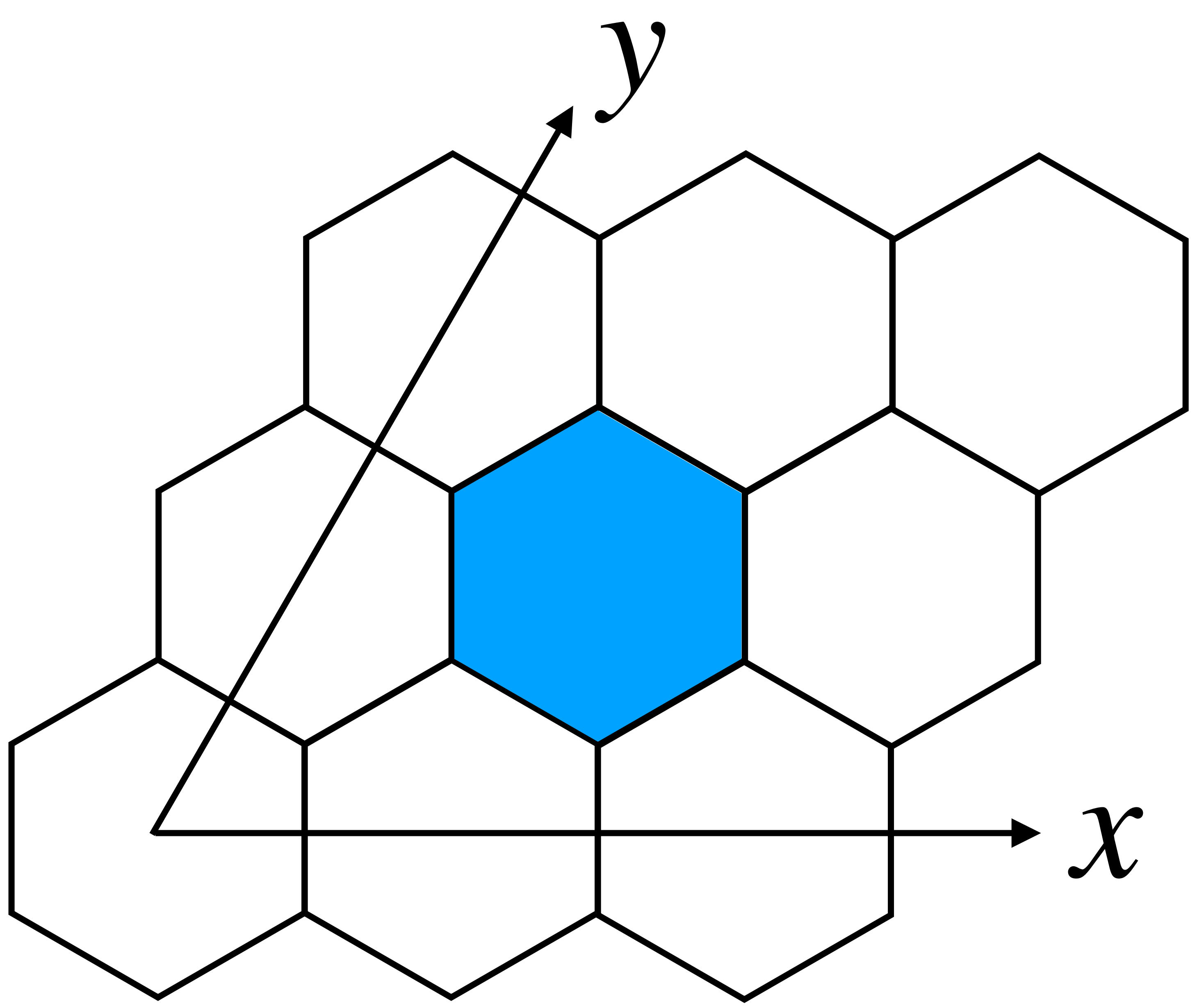


$$H_{\rm el} = \frac{g^2}{2}\frac{3\sqrt{3}}{2}\sum_{\boldsymbol{n}}\sum_{i=1}^{3} E_i^2(\boldsymbol{n})$$

$$H_{\rm mag} = -\frac{4\sqrt{3}}{9a^2g^2}\sum_{\boldsymbol{n}} \hexagon(\boldsymbol{n})$$

$\langle J_i | \hexagon | j_i \rangle$ between physical states

$=$ product of six $6j$ symbols

BM, X. Yao, PRD 108 (2023) 094505

# Spectral form factor (SFF)

$$F(t) = Z(\beta + it)Z(\beta - it)\Big|_{\beta\to 0} = \left|\mathrm{Tr}\, e^{-iHt}\right|^2 = \overline{\left|\int dE\, f(E)\,\rho(E)\, e^{-iET}\right|^2}$$

Filter function $f(E) = e^{-(E-E_0)^2/2\sigma^2}$ — small $\sigma$ enhances sensitivity to late times.

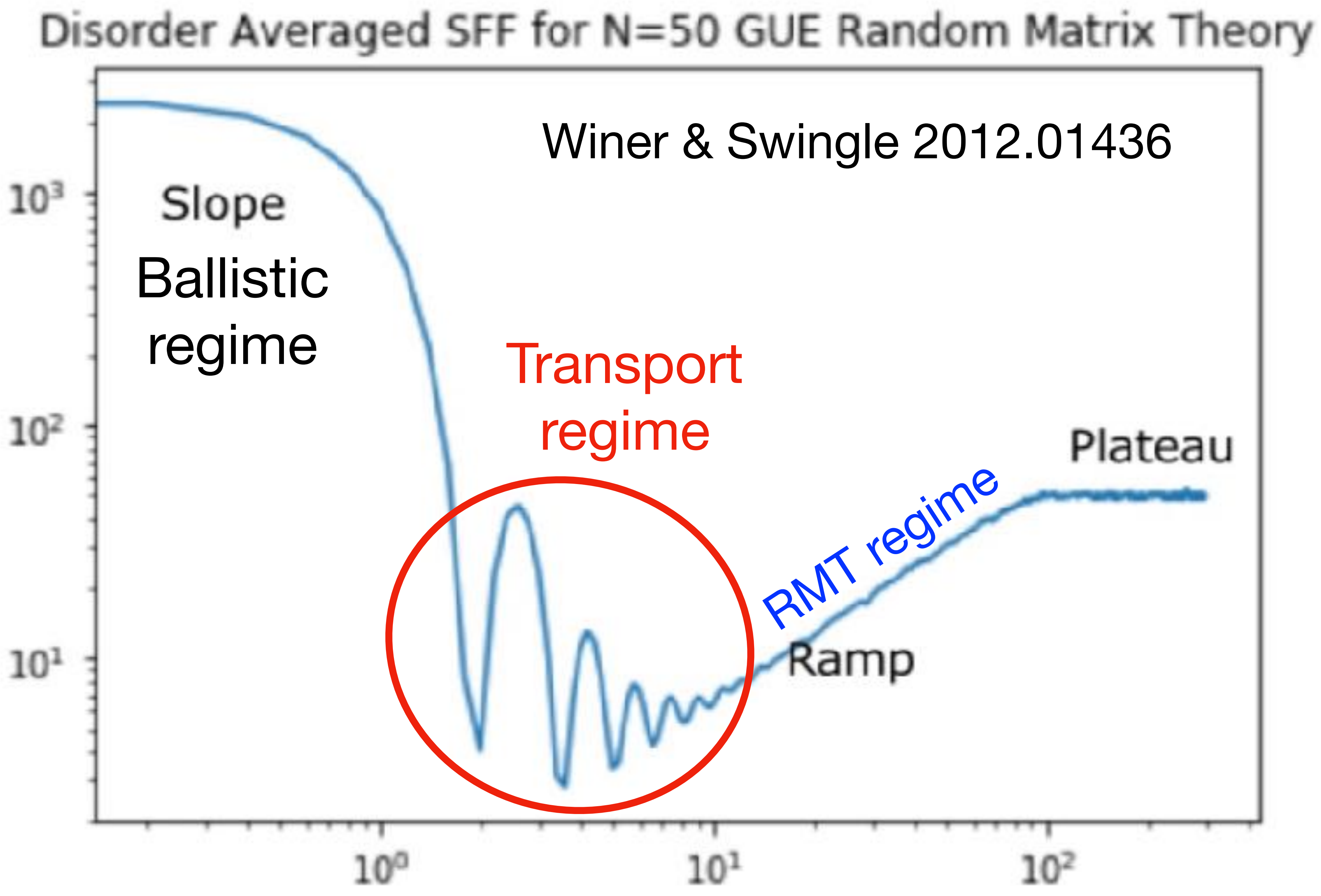


$$\mathrm{SFF}_{\mathrm{ramp}}(t) = \int dE \frac{t}{\pi\mathfrak{b}} f^2(E)$$

$\mathfrak{b}$ = Dyson index

$$\mathrm{SFF}_{\mathrm{hydro+ramp}}(t) \simeq \int dE \frac{t}{\pi\mathfrak{b}} f^2(E)\, \exp\left[\frac{V\zeta(3/2)}{(4\pi D t)^{1/2}}\right]$$

$D$ = Diffusion coefficient

In general, $\mathrm{SFF}_{\mathrm{hydro}}$ reflects a discrete spectrum of exponentially decaying transport modes

# SFF for SU(2) plaquette chain

## LGT exhibits terminal RMT behavior

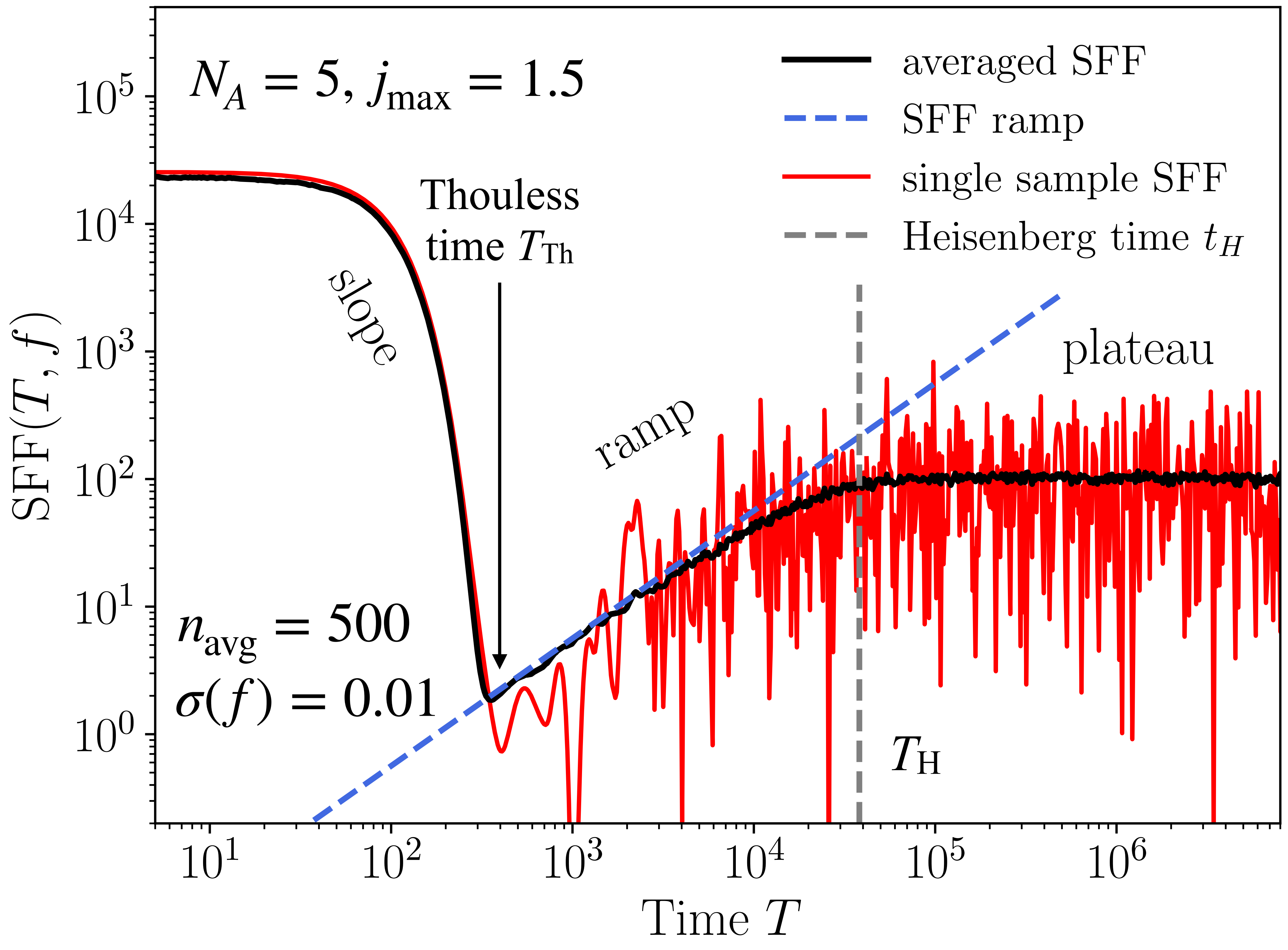


## Transport modes

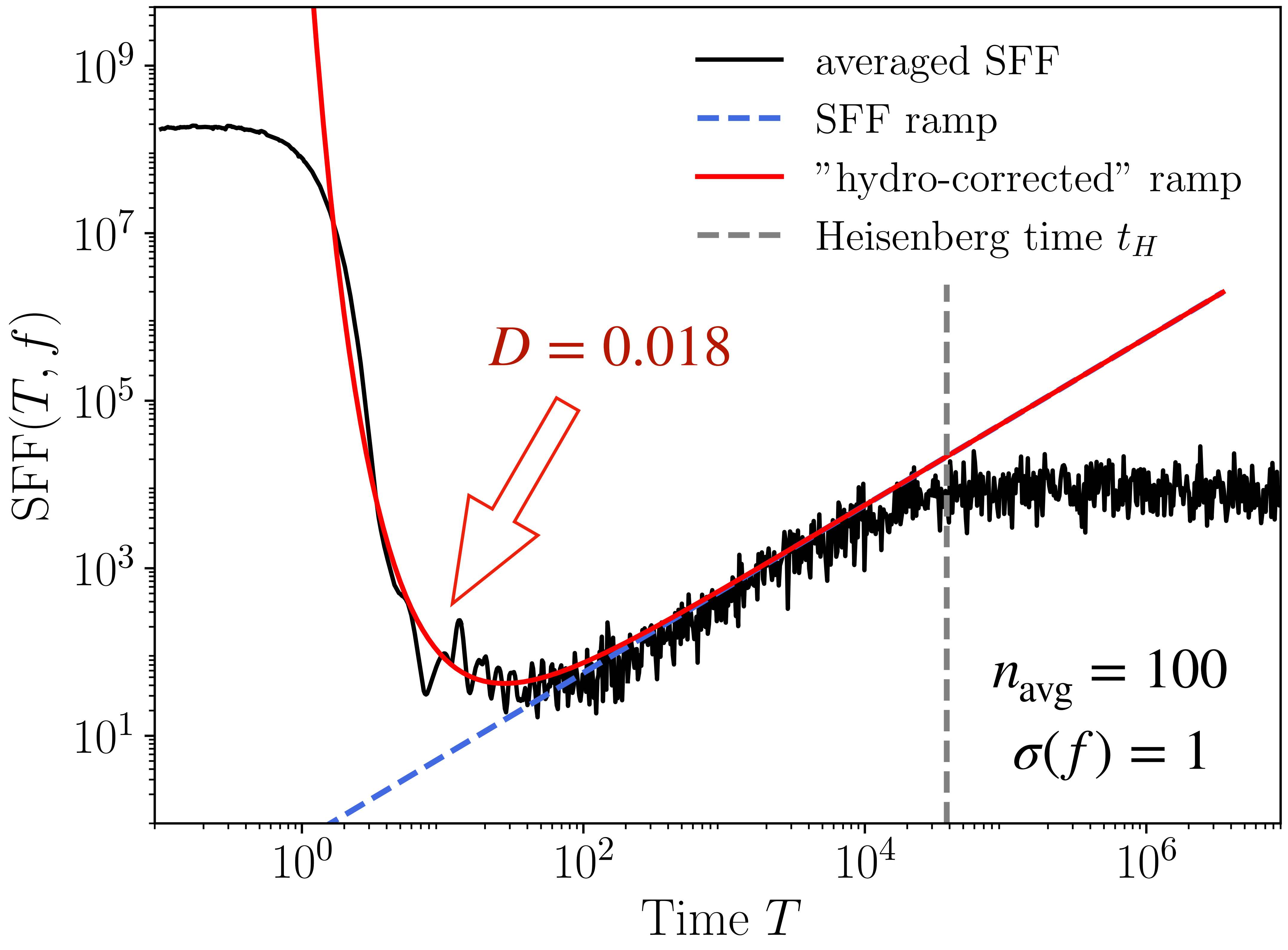


L. Ebner, BM, L. Schmotzer, A. Schäfer, C. Seidl, X. Yao, *to be published*

# Entropy concepts

Distinguish:

- Genuine entanglement entropy $S_E$ of a subsystem
- "Entropy of ignorance" $S_{sp}$ based on limited information about the subsystem

Subsystem typically defined as rapidity interval Δy.

Difference: $S_E$ follows a Page curve, $S_{sp}$ does not:

$$S_E(\Delta y) \to 0 \text{ when } \Delta y \to 2y_{\rm beam}$$

Duan et al. (2111.06475) analyzed the difference in the CGC model

But what about full QCD?

Rigorous study requires real-time dynamics of QCD. Let's begin with pure gauge theory and simplify SU(3) → SU(2) in 2 dimensions

Note: no dynamical gauge fields in one dimension (Schwinger model)

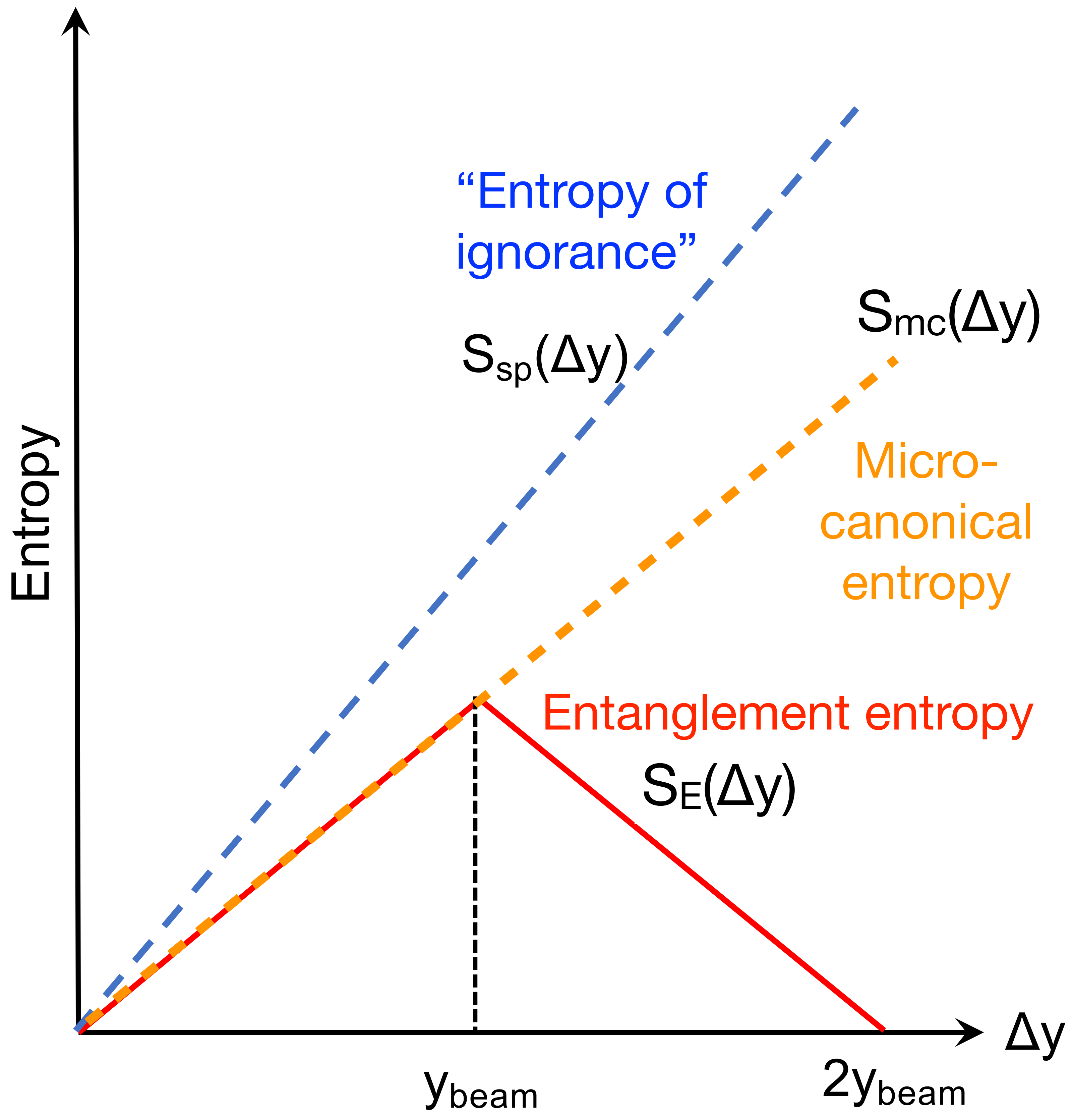

# Entanglement entropy

Page curve:

Entanglement entropy of subsystems first grows with size and then declines when the subsystem exceeds half the size of the full system [D.N. Page, PRL 71 (1993) 3743].

$$S_A = \mathrm{Tr}_A(\rho_A \ln \rho_A) \qquad \text{with} \qquad \rho_A = \mathrm{Tr}_{\bar{A}} |\psi\rangle \langle\psi|$$

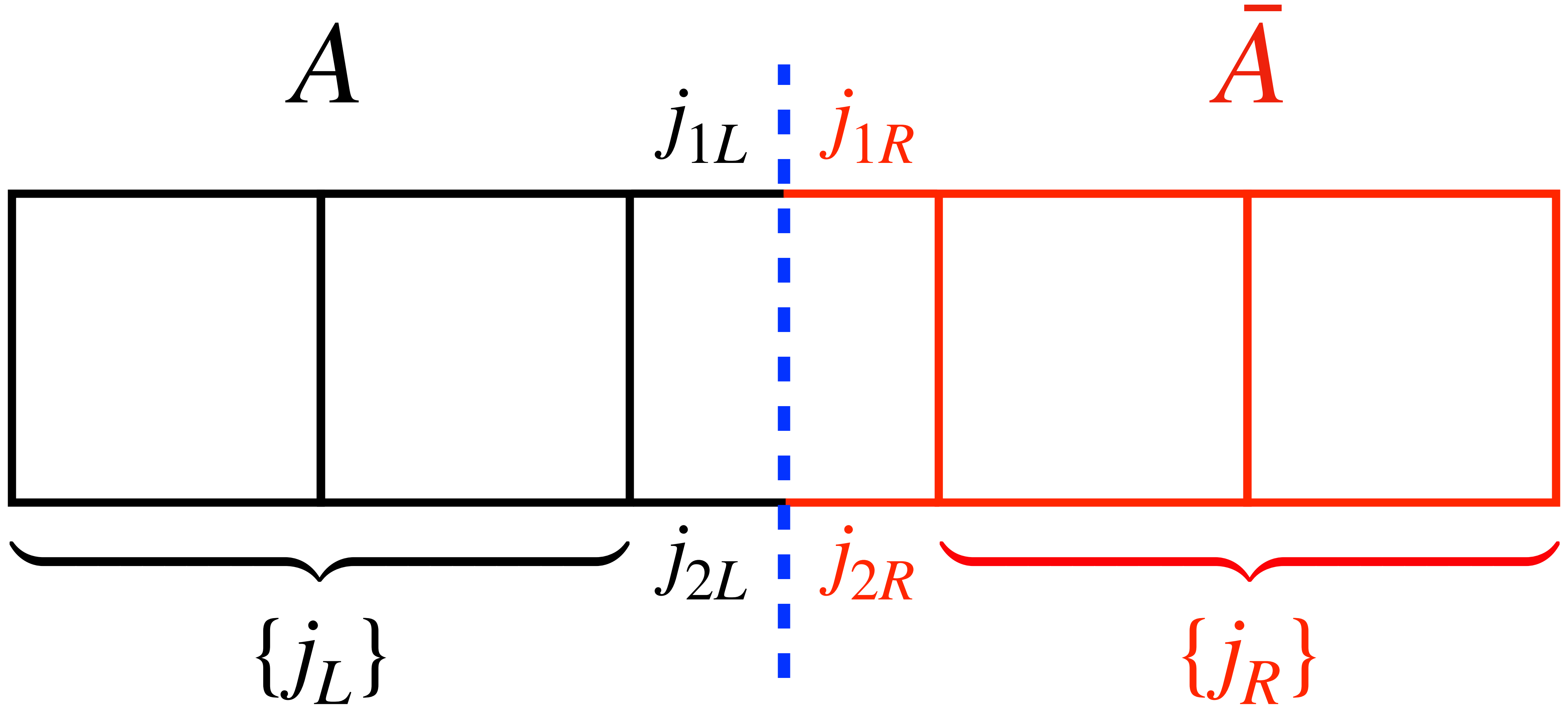


Ebner, BM, Schäfer, Seidl, Yao, 2401.15184

# Page curve

$$S(N_A) = c_0 + \frac{c}{3}\ln(c_1) + \frac{c}{3}\left[\ln[\sinh(c_1^{-1}N_A)]\theta\left(\frac{N}{2} - N_A\right) + \ln\{\sinh[c_1^{-1}(N - N_A)]\}\theta\left(N_A - \frac{N}{2}\right)\right]$$

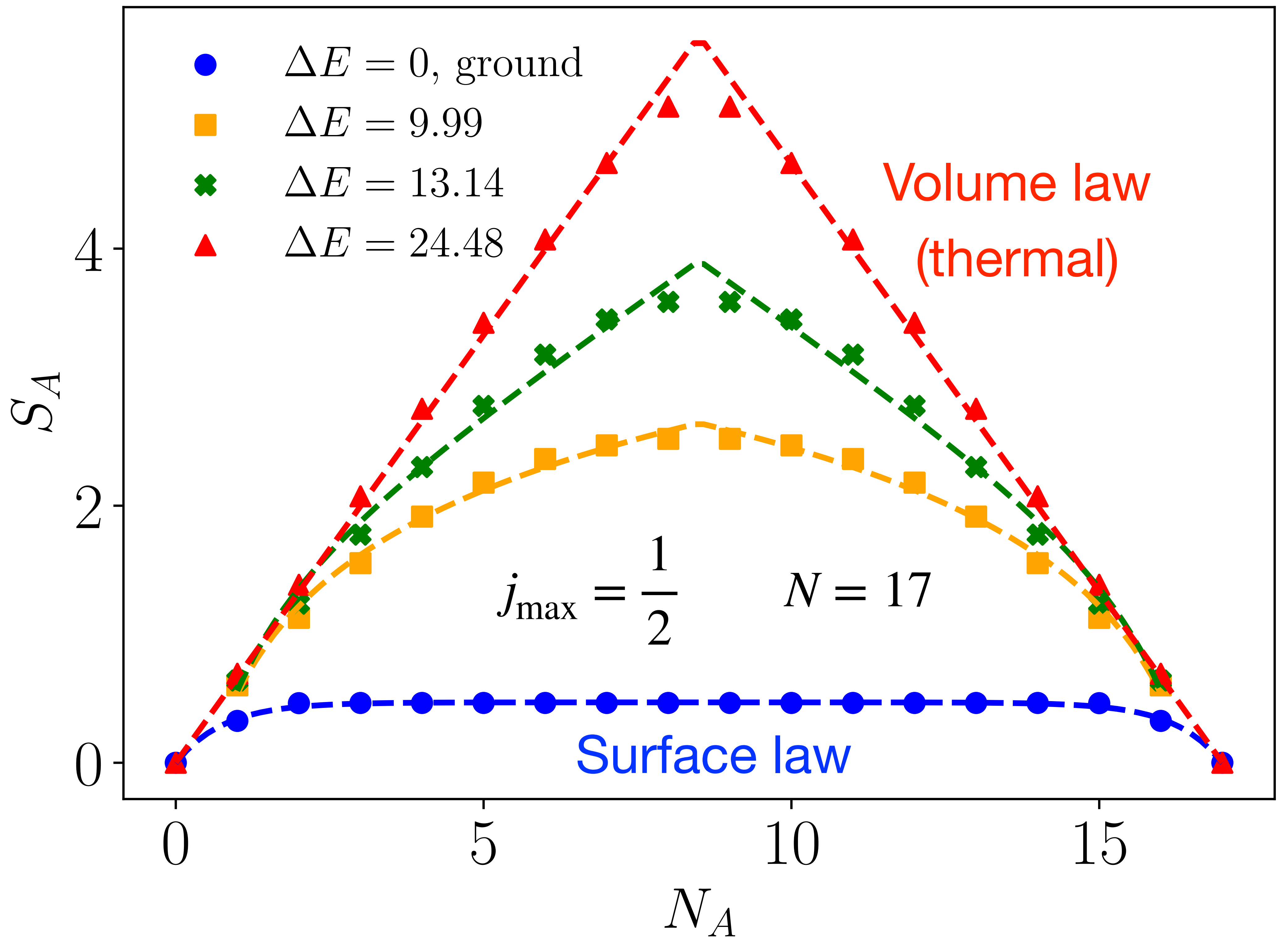


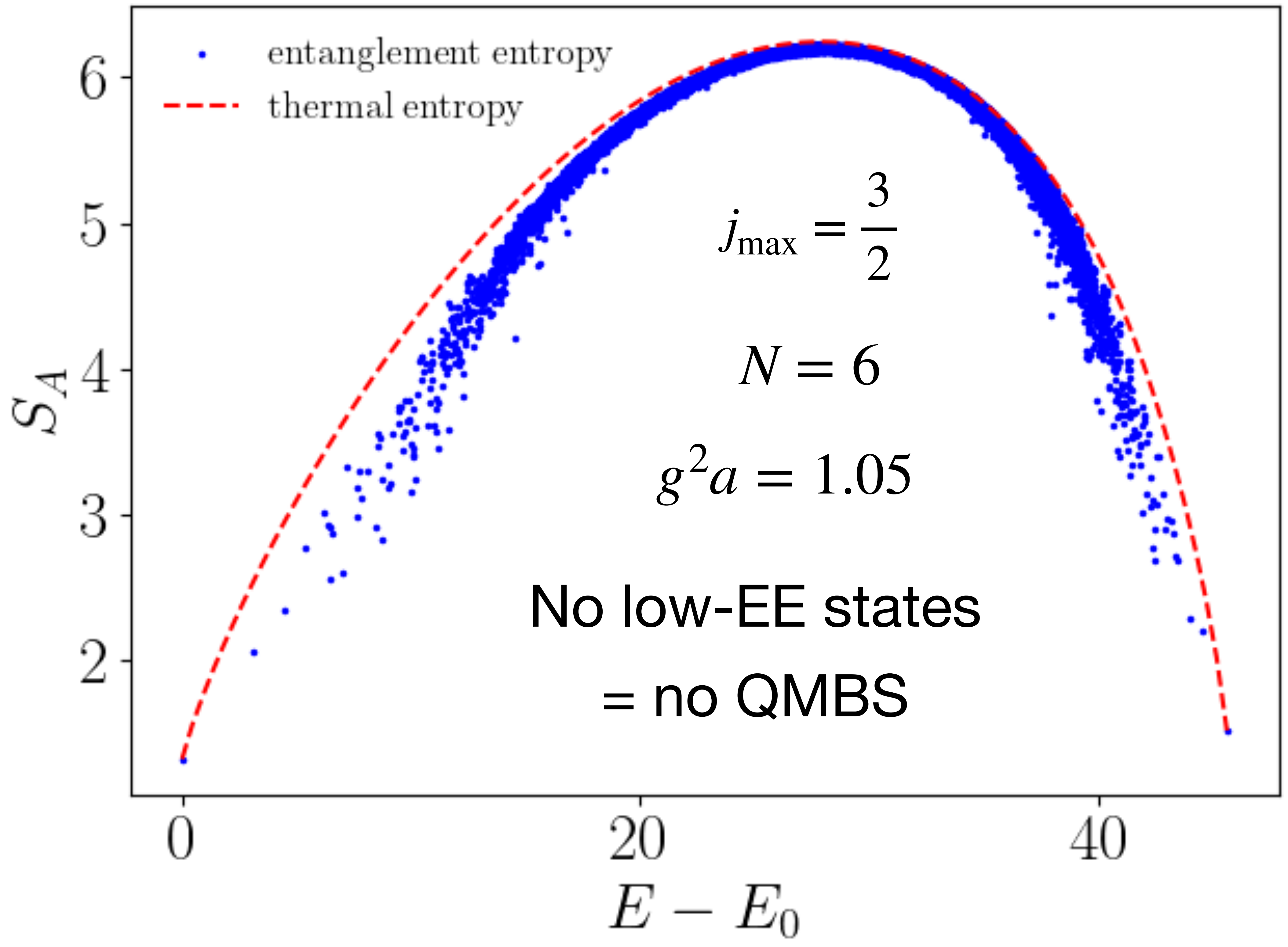


Ebner, BM, Schäfer, Seidl, Yao, *Phys.Rev.D* 110 (2024) 014505 [2401.15184]

# $S_E$ versus $S_{mc}$

$$S_{\mathrm{E}}(A) \approx \min\left(S_{\mathrm{th}}(A), S_{\mathrm{th}}(\bar{A})\right) \text{ with } T = [dS_{\mathrm{mc}}/dE]^{-1}$$

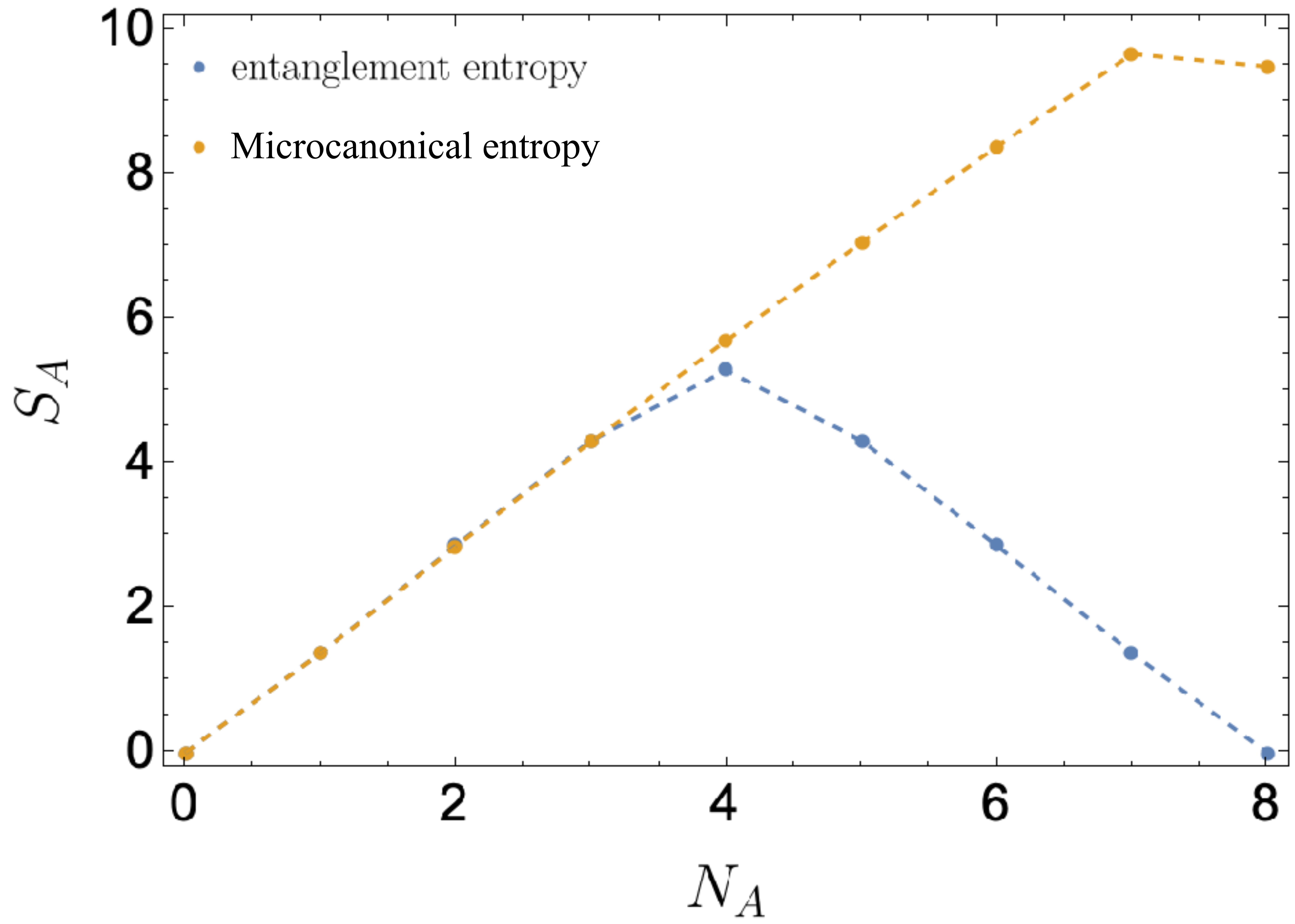


Compare with

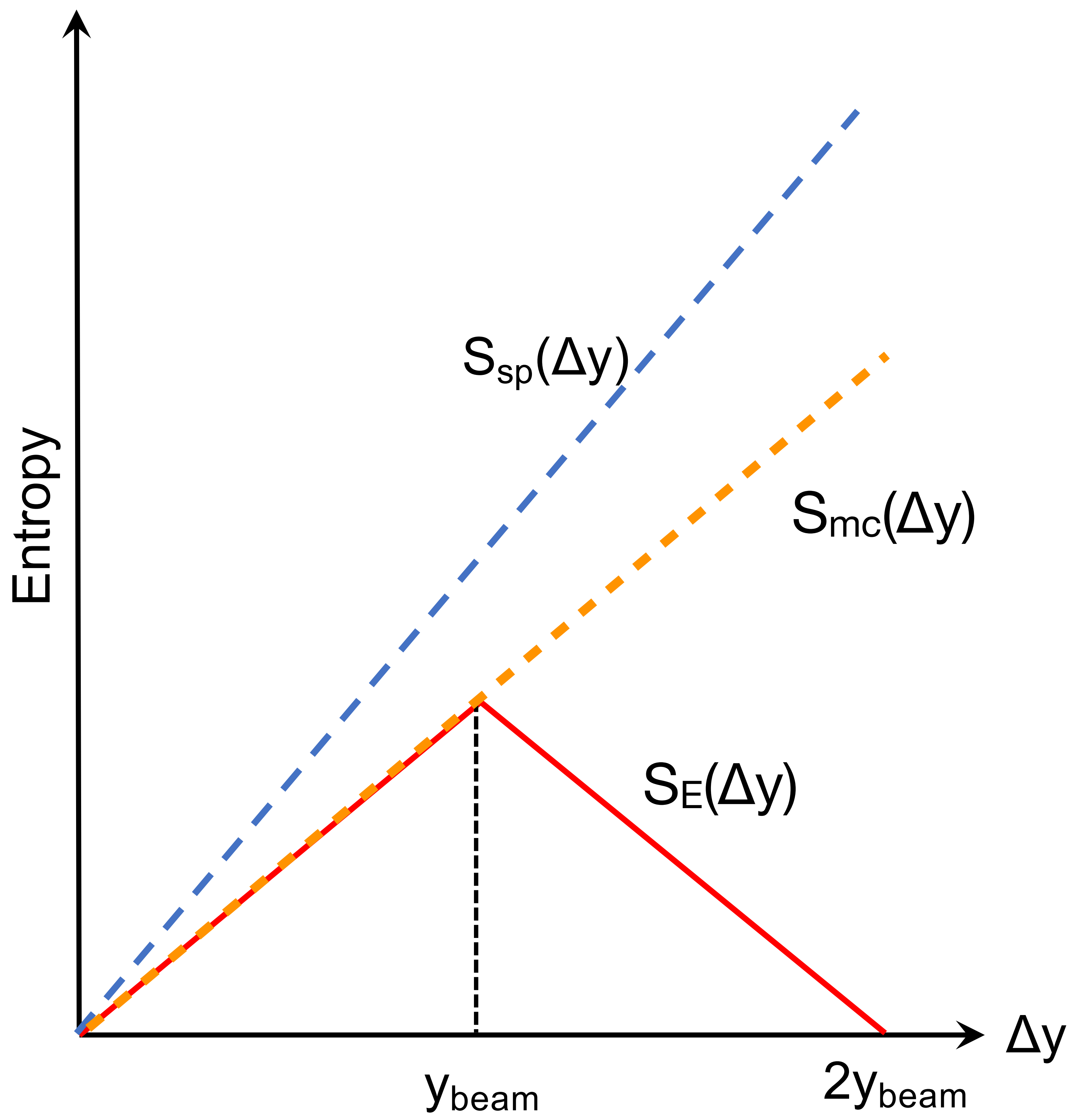

# Two-step thermalization

Step 1: Entanglement entropy introduced by local observation - depends on initial state

Step 2: Approach to micro-canonical (thermal) entropy - independent of initial state

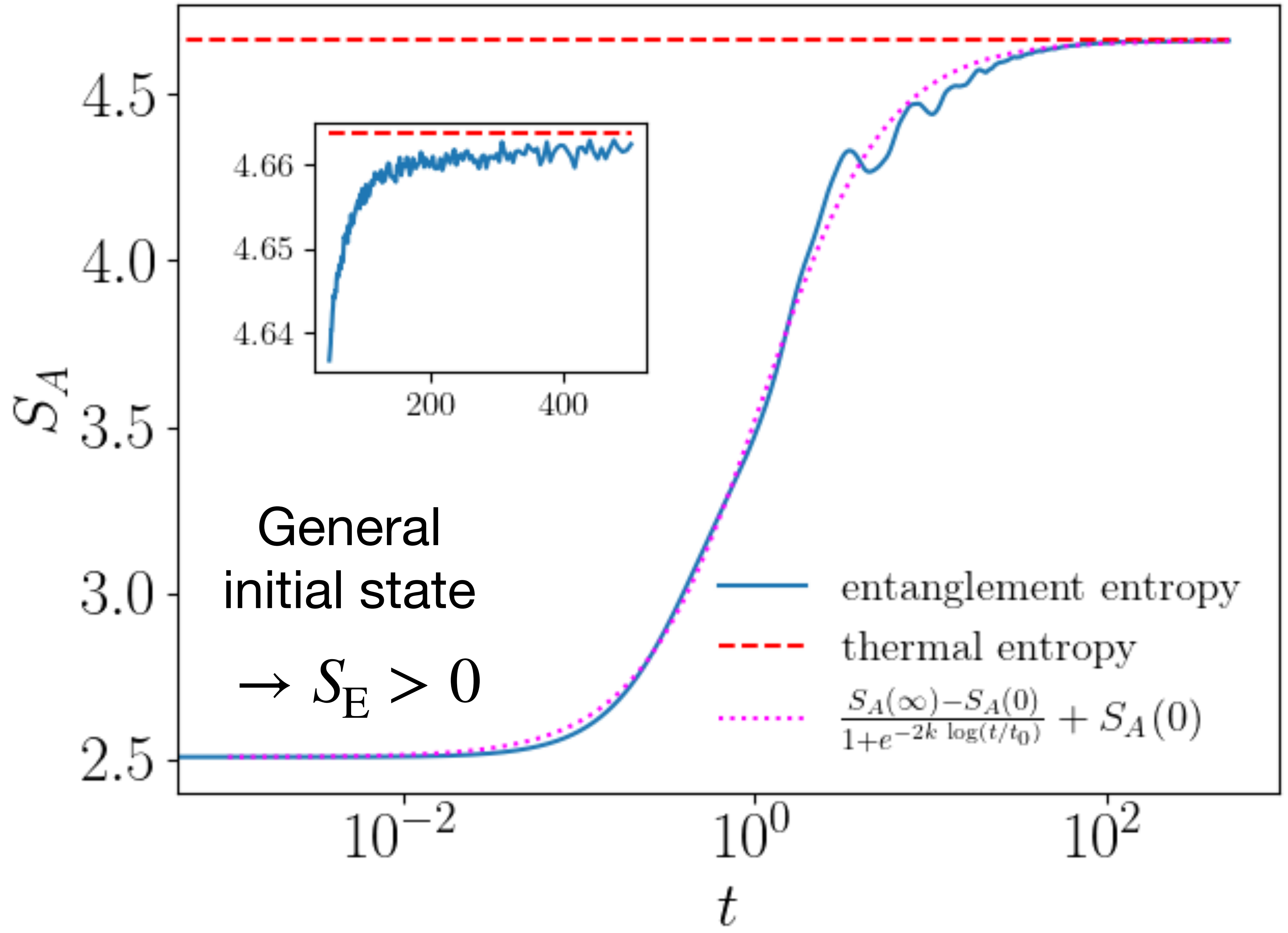


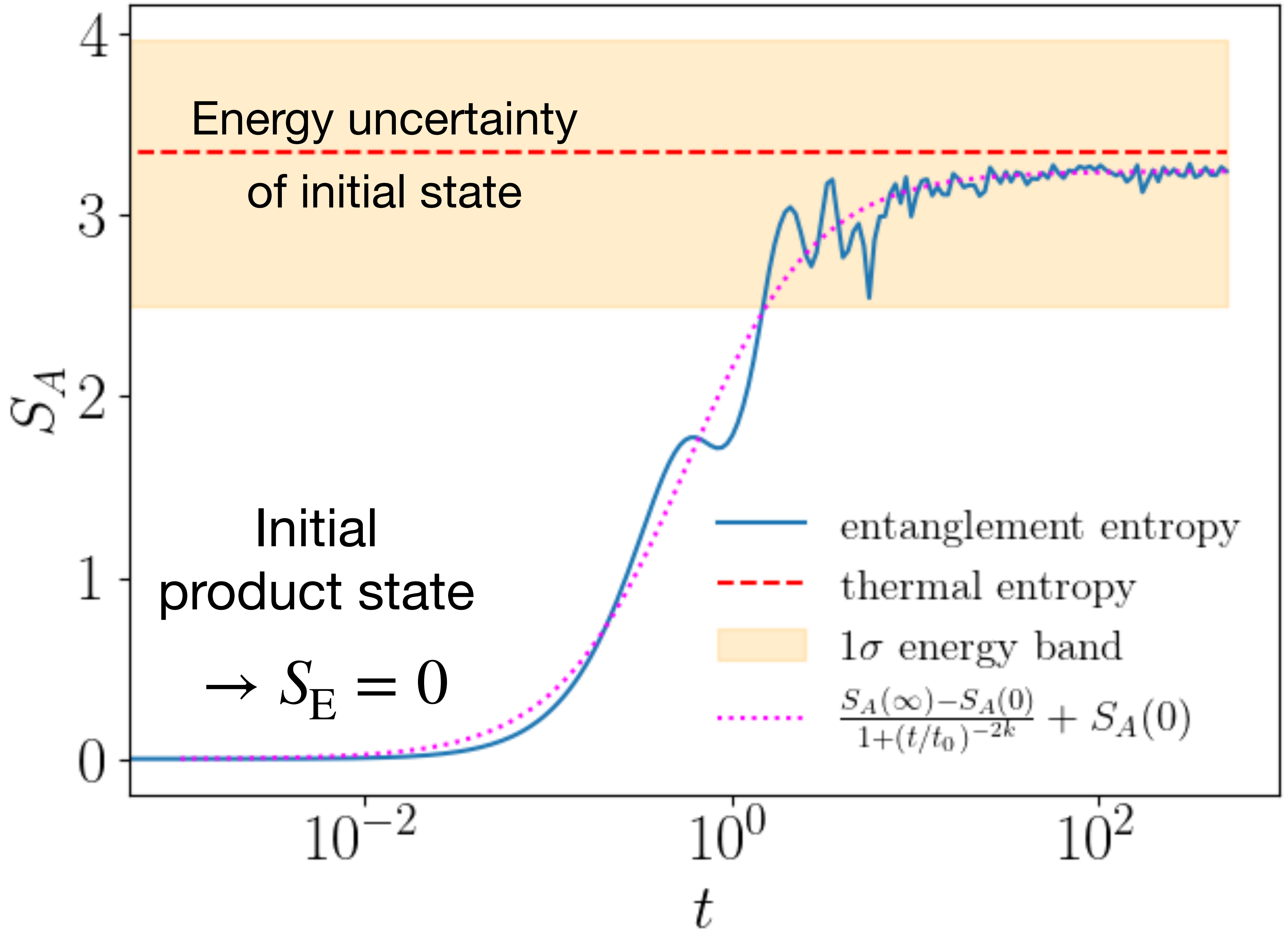


L. Ebner, BM, L. Schmotzer, A. Schäfer, C. Seidl, X. Yao, *Commun.Phys.* 8 (2025) 368 [2411.04550]

# What is “Magic”?

Unitary evolution of a quantum state can be expressed as a sequence of elementary quantum gates acting on qubits:

| Operator | Gate(s) | Matrix |
|---|---|---|
| Pauli-X (X) | X, ⊕ | $\begin{bmatrix} 0 & 1 \\ 1 & 0 \end{bmatrix}$ |
| Pauli-Y (Y) | Y | $\begin{bmatrix} 0 & -i \\ i & 0 \end{bmatrix}$ |
| Pauli-Z (Z) | Z | $\begin{bmatrix} 1 & 0 \\ 0 & -1 \end{bmatrix}$ |
| Hadamard (H) | H | $\frac{1}{\sqrt{2}}\begin{bmatrix} 1 & 1 \\ 1 & -1 \end{bmatrix}$ |
| Phase (S, P) | S | $\begin{bmatrix} 1 & 0 \\ 0 & i \end{bmatrix}$ |
| $\pi/8$ (T) | T | $\begin{bmatrix} 1 & 0 \\ 0 & e^{i\pi/4} \end{bmatrix}$ |
| Controlled Not (CNOT, CX) | • / ⊕ | $\begin{bmatrix} 1 & 0 & 0 & 0 \\ 0 & 1 & 0 & 0 \\ 0 & 0 & 0 & 1 \\ 0 & 0 & 1 & 0 \end{bmatrix}$ |

Rotation operators

$R_x(\theta), R_y(\theta), R_z(\theta),$

$$P(\varphi) = \begin{bmatrix} 1 & 0 \\ 0 & e^{i\varphi} \end{bmatrix}$$

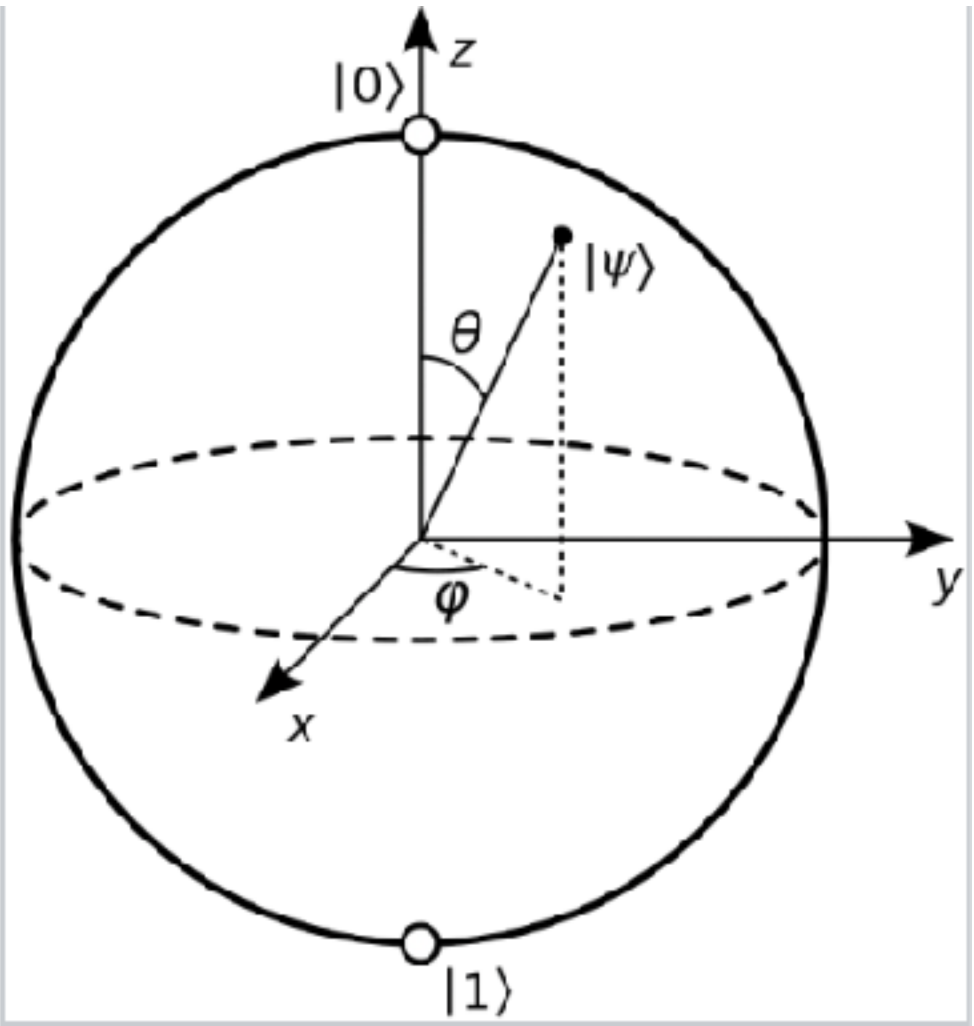

Bloch sphere of a qubit

Clifford set: {CNOT, *H*, *S*} is <u>not</u> universal

Requires an additional gate, e.g. *T*-gate

# Gottesman-Knill theorem (1998)

Quantum circuits consisting solely of operators from the Clifford group (Pauli matrices *I, X, Y, Z*) or equivalently the Clifford gate set {CNOT, *H, S*} can be perfectly simulated in polynomial time by a probabilistic digital computer.

Such quantum circuits are called "stabilizer" circuits. The amount of *non-stabilizer* quantum resources, such as *T*-gates, required to implement a unitary evolution is called *non-stablizerness* or "**magic**".

The quantitative determination of the "magic" resources required by a quantum evolution is difficult.

A lower limit is provided by the stabilizer Rényi entropies, i.e. Clifford averaged Rényi entropies:

$$M_n(\rho) = \frac{1}{1-n} \log \left[ \sum_{P \in \mathcal{P}_N} 2^{-N} |\mathrm{Tr}(\rho P)|^{2n} \right]$$

Linearized: $M_2(\rho) = -\log[1 - M_{\mathrm{lin}}(\rho)]$

**Anti-flatness** of the entanglement spectrum of a subsystem *A*: $\mathcal{F}_A(\rho) = \mathrm{Tr}(\rho_A^3) - [\mathrm{Tr}(\rho_A^2)]^2$

$$\langle \mathcal{F}(\rho) \rangle_{\mathcal{P}} \propto M_{\mathrm{lin}}(\rho)$$

[E. Tirrito et al., PRA 109 (2024) L040401 [2304.01175]

# Anti-flatness

The *entanglement spectrum* of a density matrix is the spectrum of its *entanglement Hamiltonian*:

$$\rho = e^{-\tilde{H}} \quad \leftrightarrow \quad \tilde{H}|\nu\rangle = \omega_\nu |\nu\rangle$$

Examples of **flat** entanglement spectrum: Pure state: $\rho = |\psi\rangle\langle\psi| \quad \rightarrow \quad \omega_1 = 0, \omega_{\nu>1} = N$

Maximally mixed state: $\rho = \frac{1}{N} I_N \quad \rightarrow \quad \omega_\nu = \log N$

During (local) thermalization of a pure state, the reduced density matrix $\rho_A$ first steepens and later flattens out again as the reduced density matrix becomes quasi-thermal and maximally mixed.

Maximal anti-flatness is reached during period of maximal entanglement entropy growth = time of most rapid thermalization.

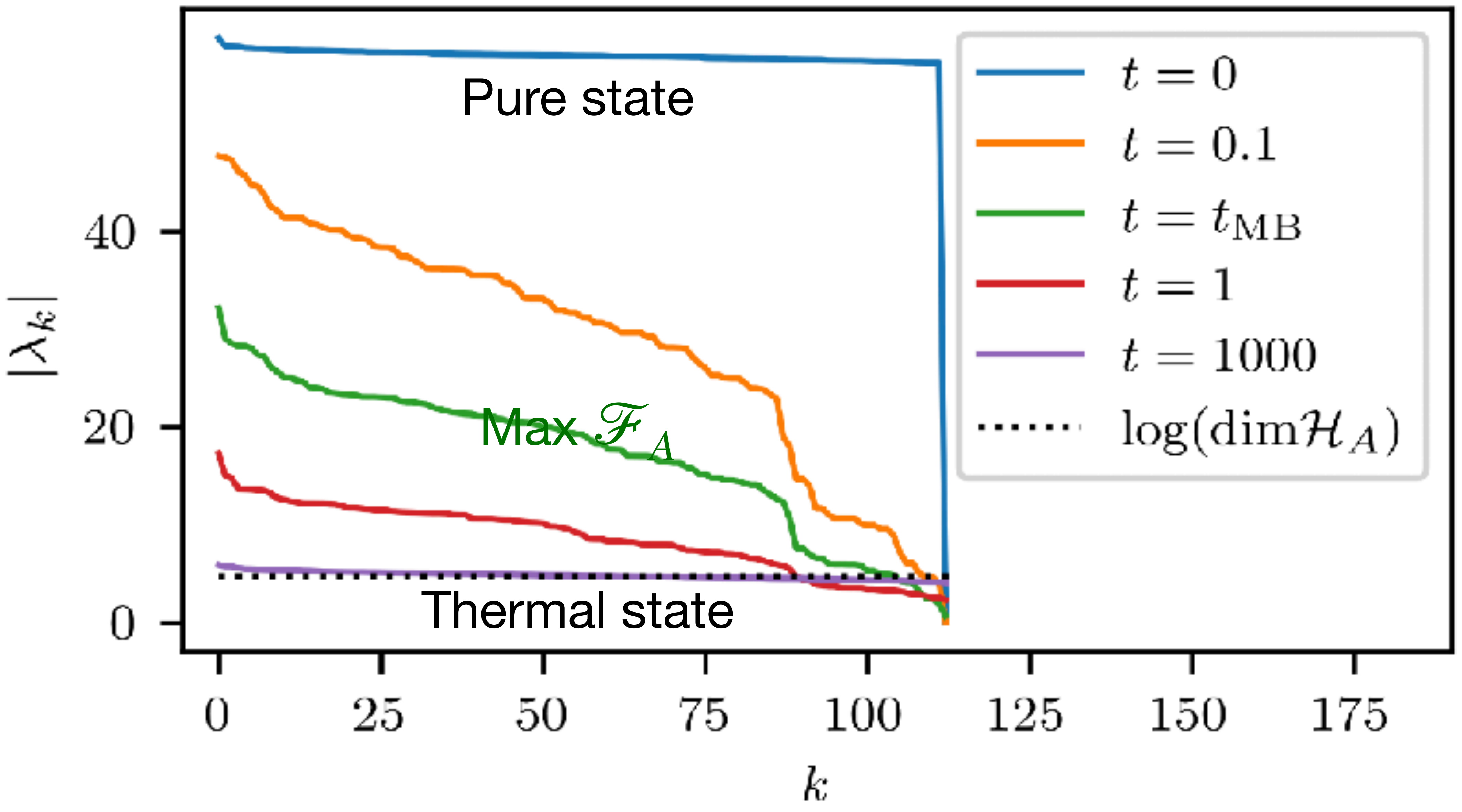

# Results for SU(2) plaquette chain

[L. Ebner *et al.*, 2510.11681]

SU(2) on 7-plaquette chain

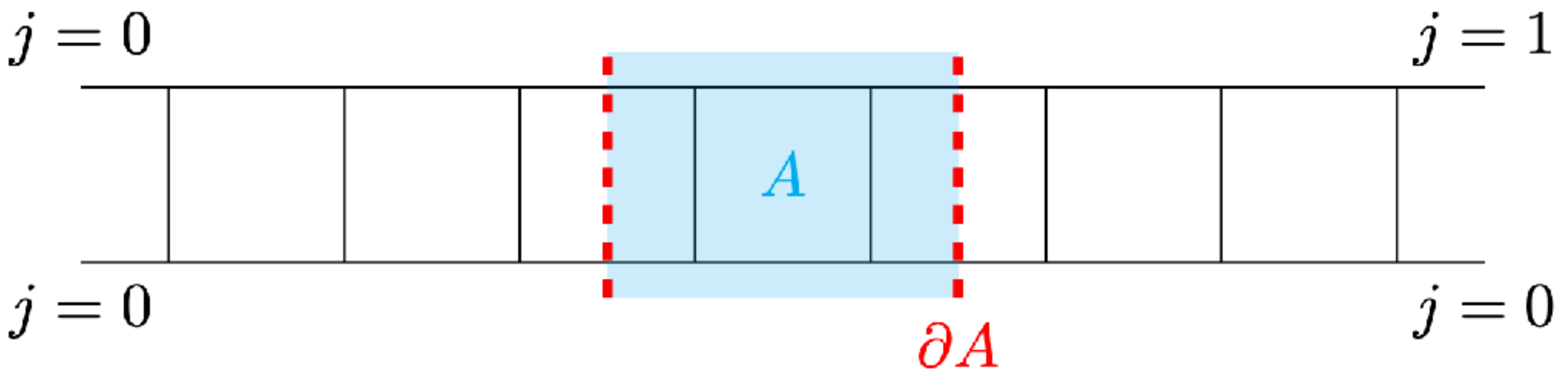


External links of subsystem act like surface charges; they give incoherent contribution to $S_E$.

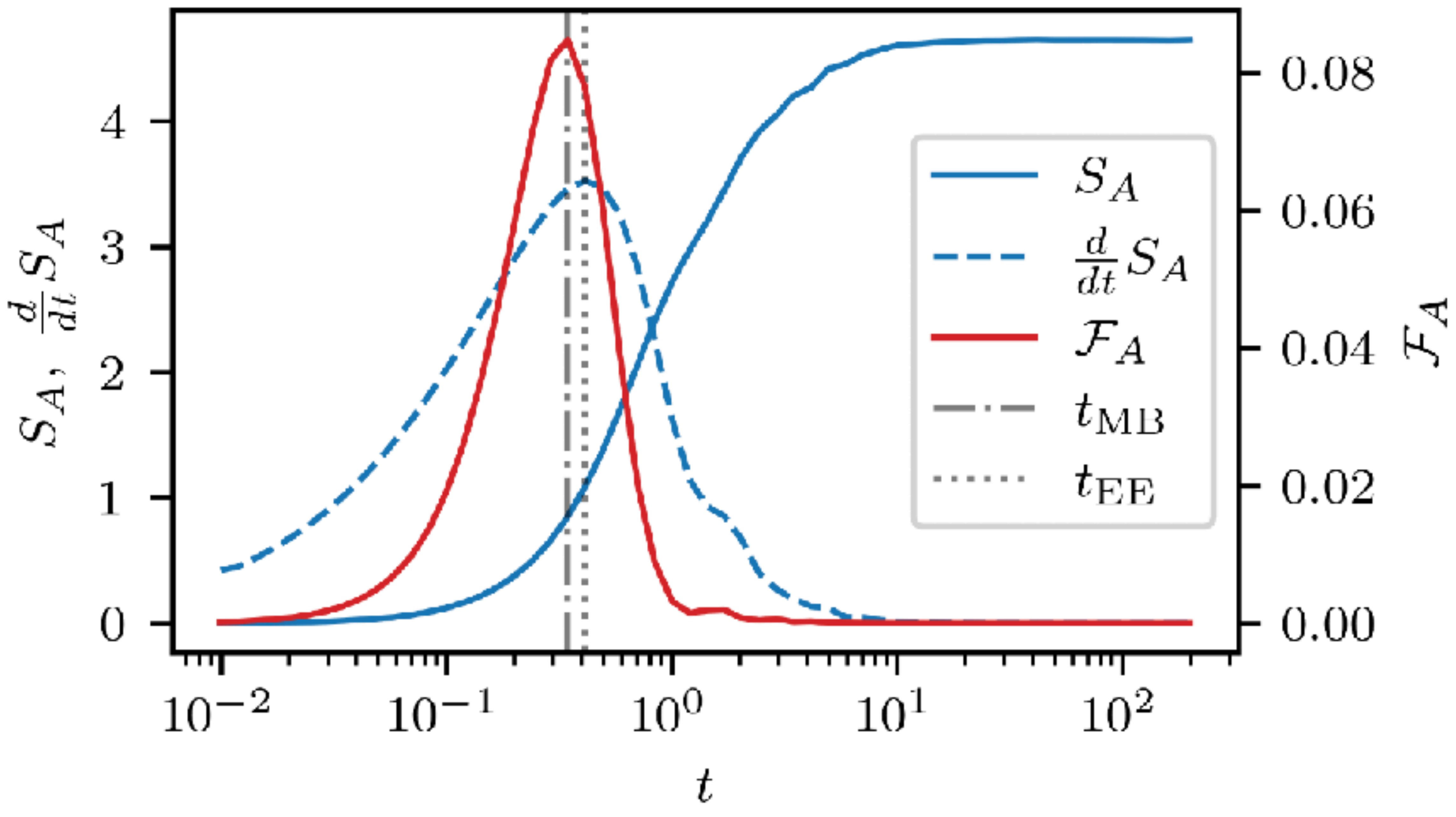


Initial state: Highly excited product state of electric energy on links obeying Gauss law. Can be thought of strong coupling eigenstate.

Anti-flatness peaks precisely where the growth rate of the entanglement entropy is maximal, i.e. when quantum correlations are rapidly rearranged.

# Results II

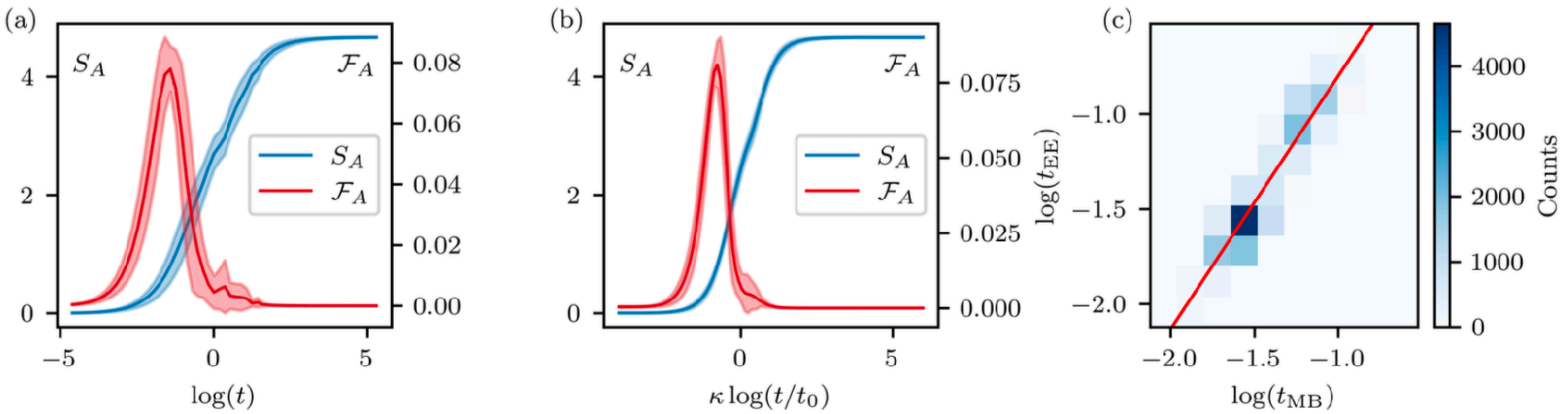


(b) Rescaled time evolution, where the time t is replaced by κ log($t/t_0$) with state-dependent parameters κ and $t_0$, such that the thermalization of different states is synchronized.

(c) Joint distribution of magic barrier time $t_{MB}$ and time of maximum entanglement entropy growth $t_{EE}$ on a logarithmic scale for all 18389 electric basis states satisfying the Gauss law.

# Results III

Coupling dependence of entanglement dynamics

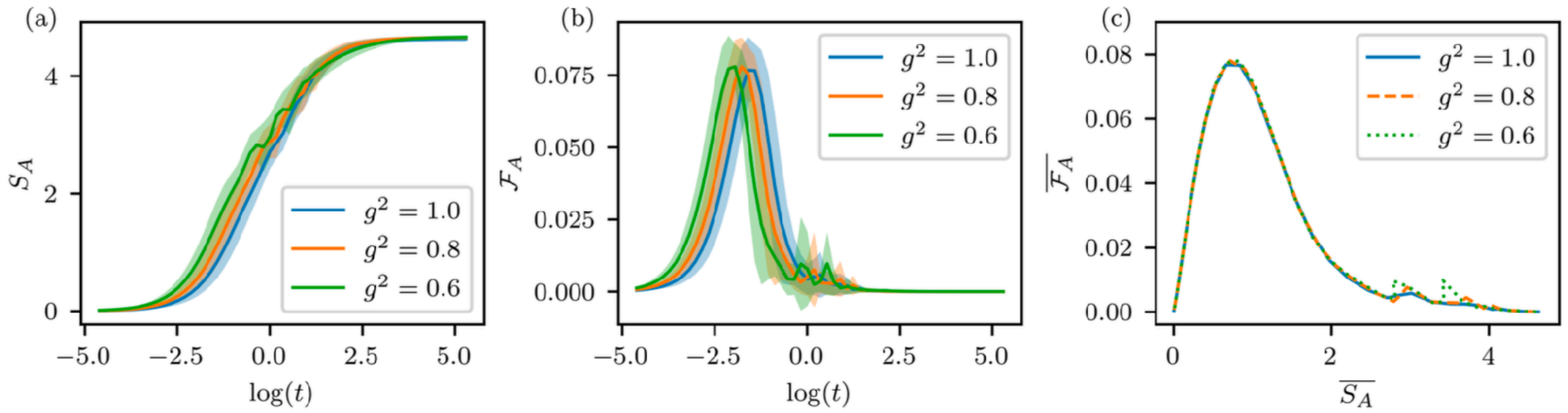


(c) Parametric dependence of $\mathscr{F}_A$ on $S_A$ for different ergodic couplings

The behavior seems to be universal for ergodic quantum systems; it is seen also in the transverse field Ising model.

# SU(3)

KS Hamiltonian: $$H = \frac{g^2\Sigma}{n_l}\sum_{\text{links}}(E_i^a)^2 + \frac{1}{g^2\Sigma}\sum_{\text{plaq}}(6 - U_P - U_P^\dagger)$$

Square lattice $n_l = 2,\ \Sigma = 1$

Hexagonal lattice $n_l = 3,\ \Sigma = \frac{3\sqrt{3}}{2}$

Representations: Singlet

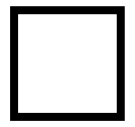
$3$ = quark

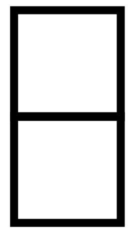
$\overline{3}$ = quark

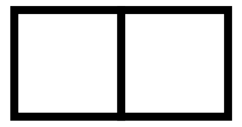
$6$ = di-quark

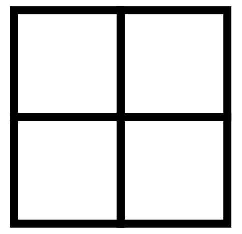
$\overline{6}$ = di-quark

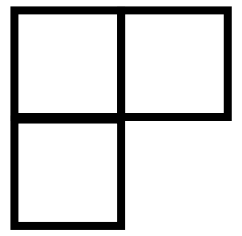
$8$ = gluon

Minimal truncation of SU(3) gauge group

With this truncation, SU(3) on linear square plaquette chains or hexagonal ("honeycomb") lattices can formulated as a quantum theory of qutrits (= a type of *N* = *3* Potts model).

# Plaquette operator matrix

| $P_L$ \ $P_R$ | 0 | 1 | 2 |
|---|---|---|---|
| 0 | $\begin{pmatrix} 0 & 1 & 1 \\ 1 & 0 & 1 \\ 1 & 1 & 0 \end{pmatrix}$ | $\begin{pmatrix} 0 & 1 & 1 \\ \frac{1}{3} & 0 & \frac{1}{\sqrt{3}} \\ \frac{1}{\sqrt{3}} & 1 & 0 \end{pmatrix}$ | $\begin{pmatrix} 0 & 1 & 1 \\ \frac{1}{\sqrt{3}} & 0 & 1 \\ \frac{1}{3} & \frac{1}{\sqrt{3}} & 0 \end{pmatrix}$ |
| 1 | $\begin{pmatrix} 0 & \frac{1}{3} & \frac{1}{\sqrt{3}} \\ 1 & 0 & 1 \\ 1 & \frac{1}{\sqrt{3}} & 0 \end{pmatrix}$ | $\begin{pmatrix} 0 & 1 & 1 \\ 1 & 0 & 1 \\ 1 & 1 & 0 \end{pmatrix}$ | $\begin{pmatrix} 0 & \frac{1}{\sqrt{3}} & 1 \\ 1 & 0 & 1 \\ \frac{1}{\sqrt{3}} & \frac{1}{3} & 0 \end{pmatrix}$ |
| 2 | $\begin{pmatrix} 0 & \frac{1}{\sqrt{3}} & \frac{1}{3} \\ 1 & 0 & \frac{1}{\sqrt{3}} \\ 1 & 1 & 0 \end{pmatrix}$ | $\begin{pmatrix} 0 & 1 & \frac{1}{\sqrt{3}} \\ \frac{1}{\sqrt{3}} & 0 & \frac{1}{3} \\ 1 & 1 & 0 \end{pmatrix}$ | $\begin{pmatrix} 0 & 1 & 1 \\ 1 & 0 & 1 \\ 1 & 1 & 0 \end{pmatrix}$ |

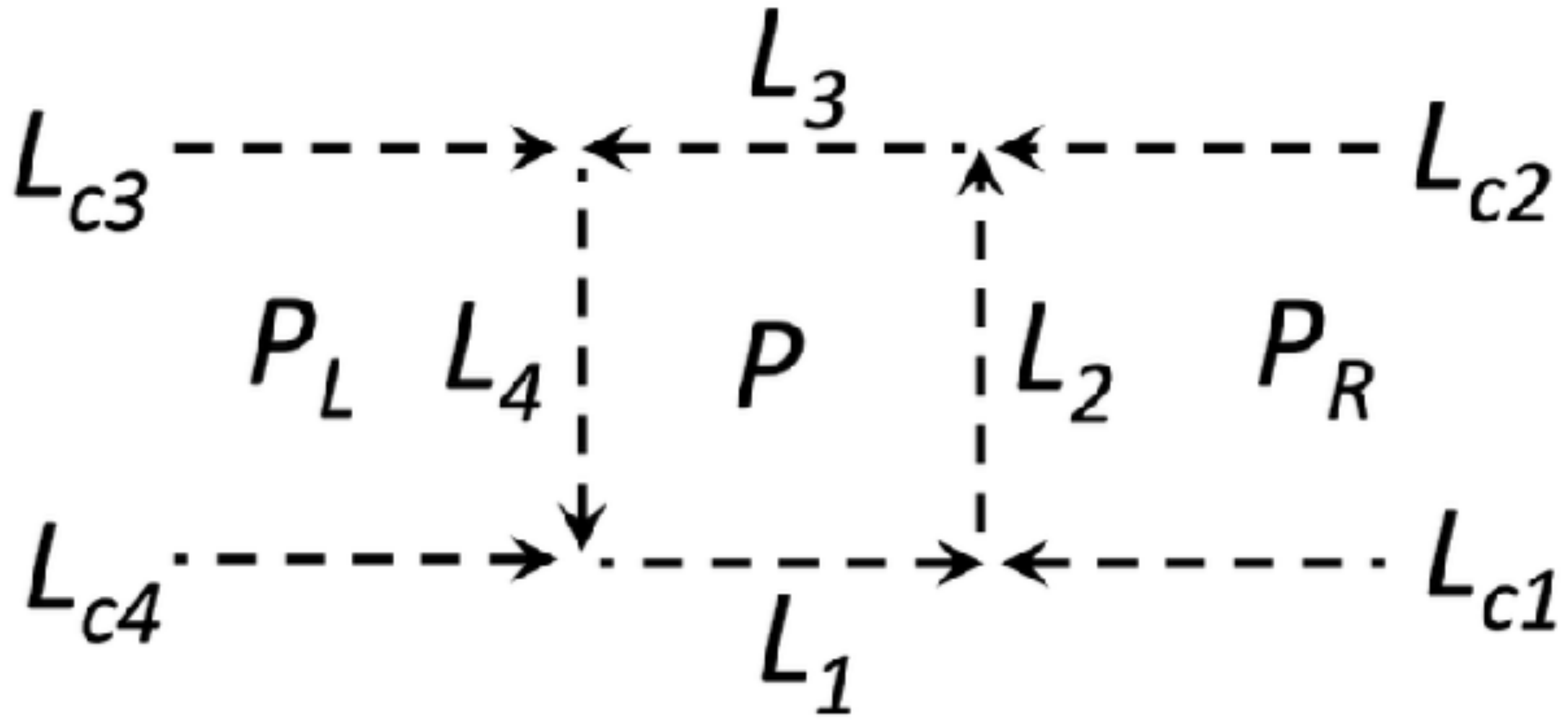


$|0\rangle$ = singlet

$|1\rangle$ = triplet

$|2\rangle$ = antitriplet

A similar, but larger, set of matrix elements can be readily worked out for the honeycomb lattice

# SU(3) LGT is chaotic

Energy gap ratio: $$r_\alpha = \frac{\min[\delta_\alpha, \delta_{\alpha-1}]}{\max[\delta_\alpha, \delta_{\alpha-1}]} \leq 1$$

GOE prediction: $$P_{\mathrm{GOE}}(r) = \frac{27}{4}\frac{r+r^2}{(1+r+r^2)^{5/2}}$$

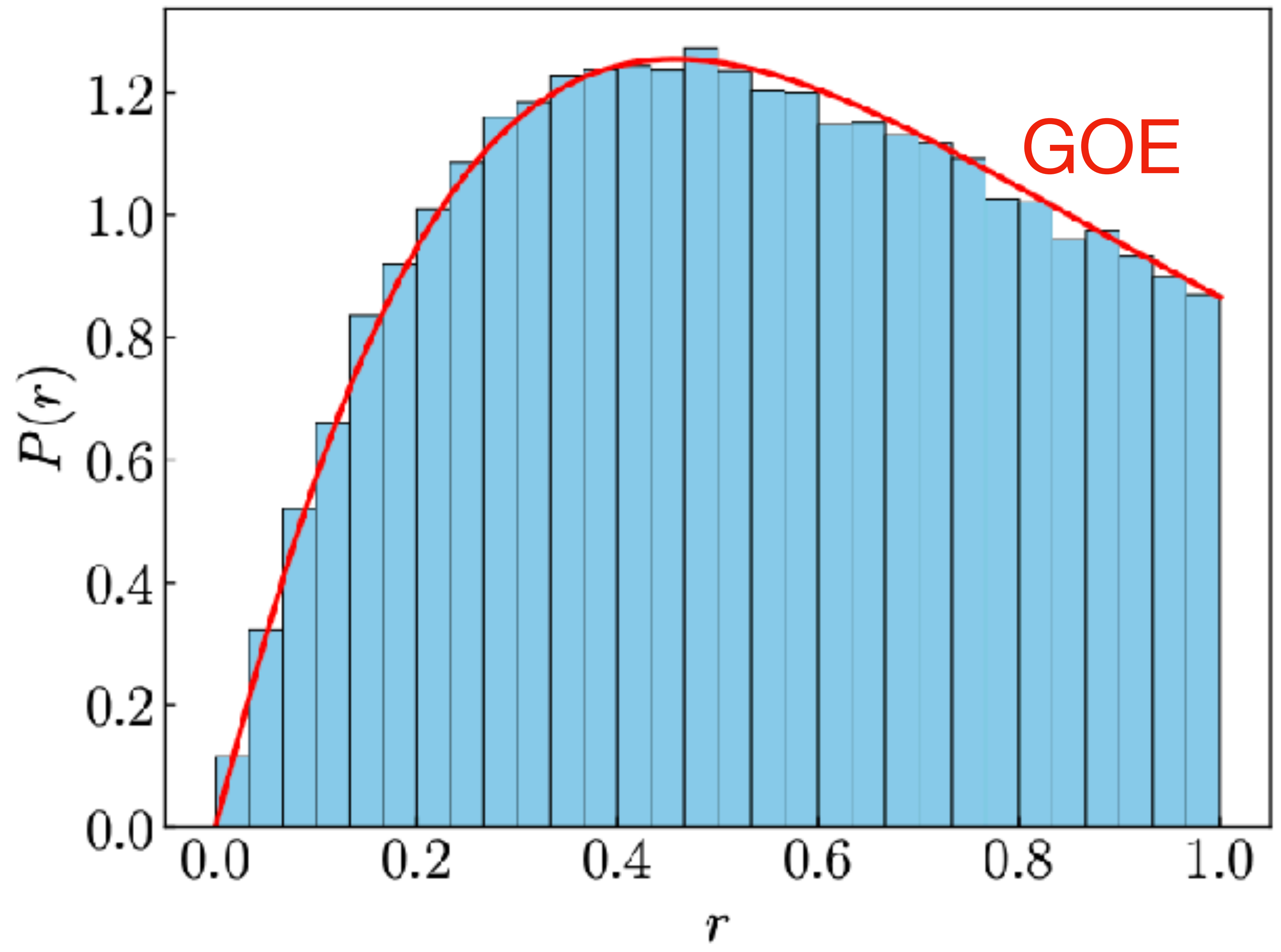


SU(3) is quantum chaotic in the physically relevant regime of weak coupling, even for for truncated theory on a short chain.

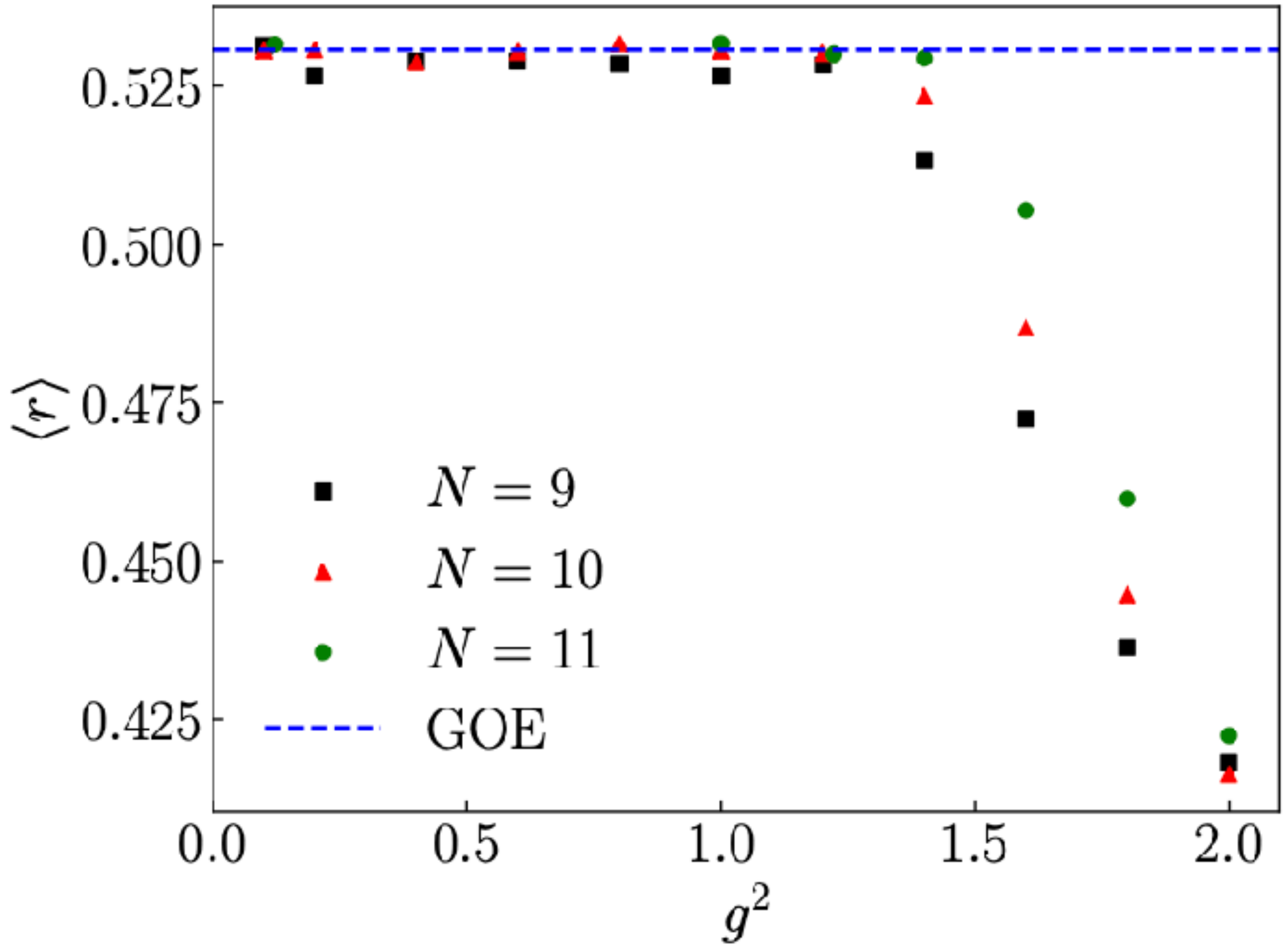

# Ground state energy gap

The ground state energy gap (“glue ball mass”) has a well defined large volume limit.

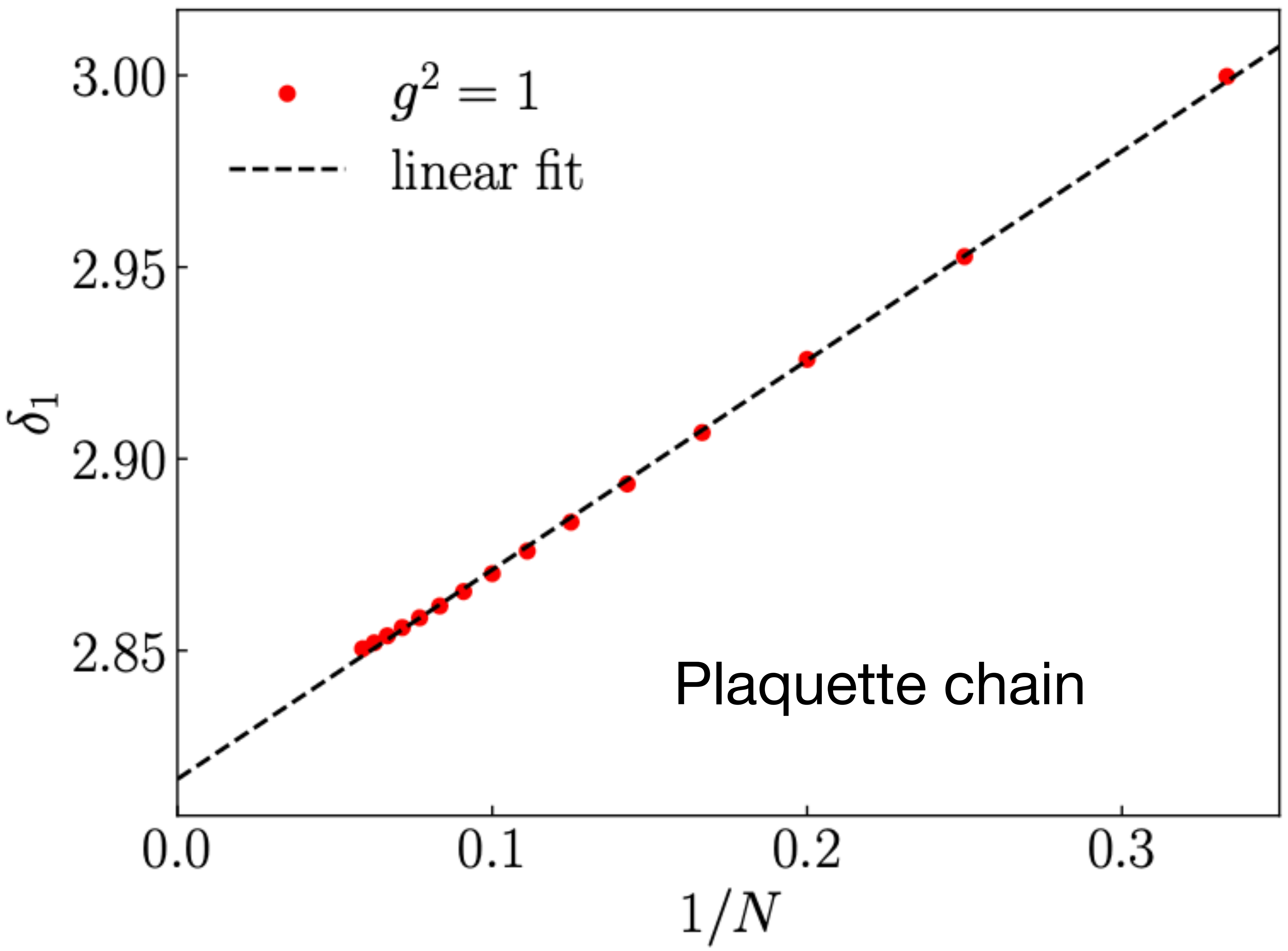


The ground state energy gap has the expected coupling constant scaling ($g_s^2 = g^2\Sigma$, $\beta_s = 3/g_s^2$).

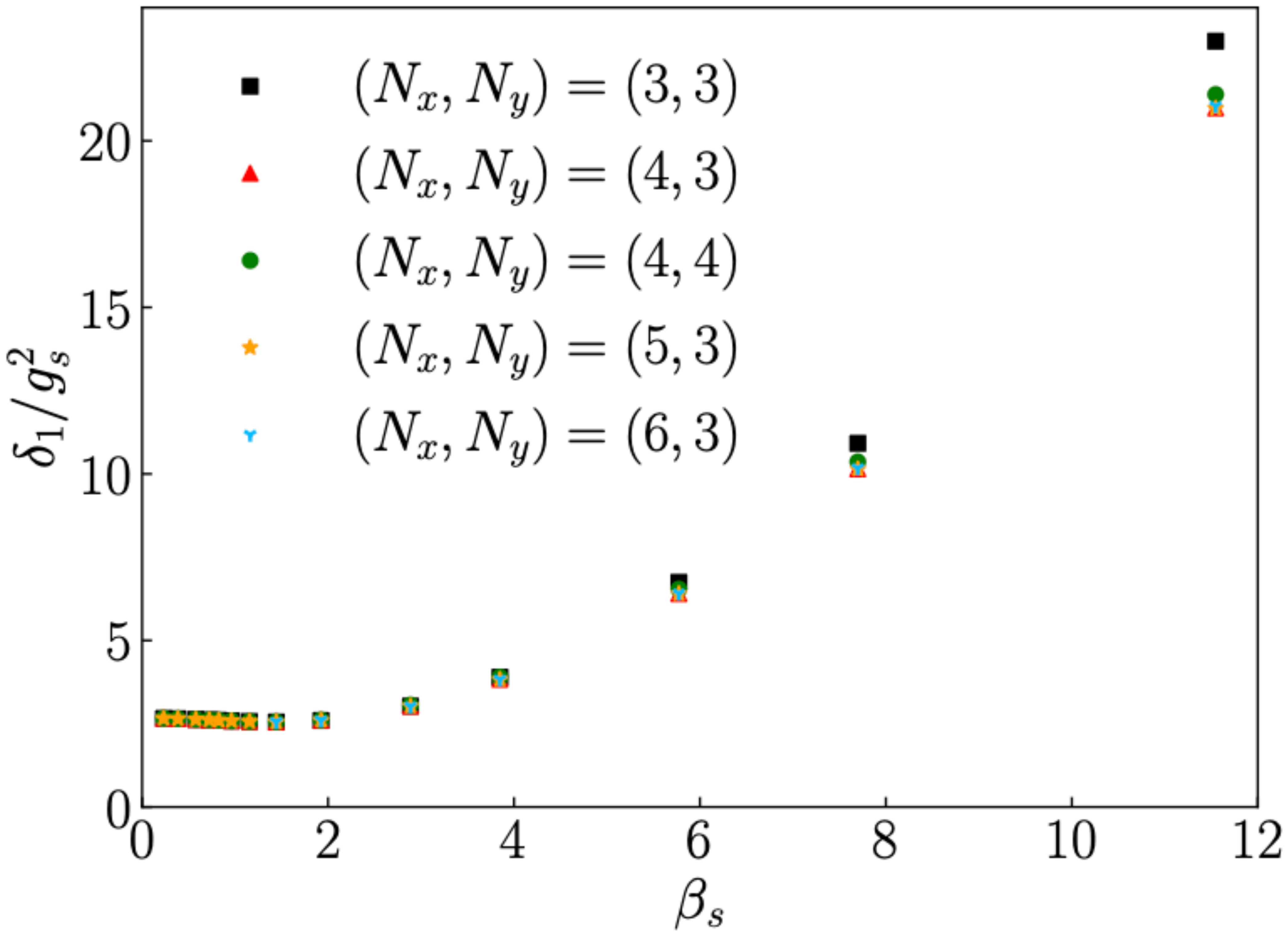

# $Q\overline{Q}$ potential

Confining potential $V_{Q\overline{Q}}(r) = \sigma r$ has finite coupling corrections from quantum fluctuations of the linear flux tube; these can be understood as virtual glue ball excitations.

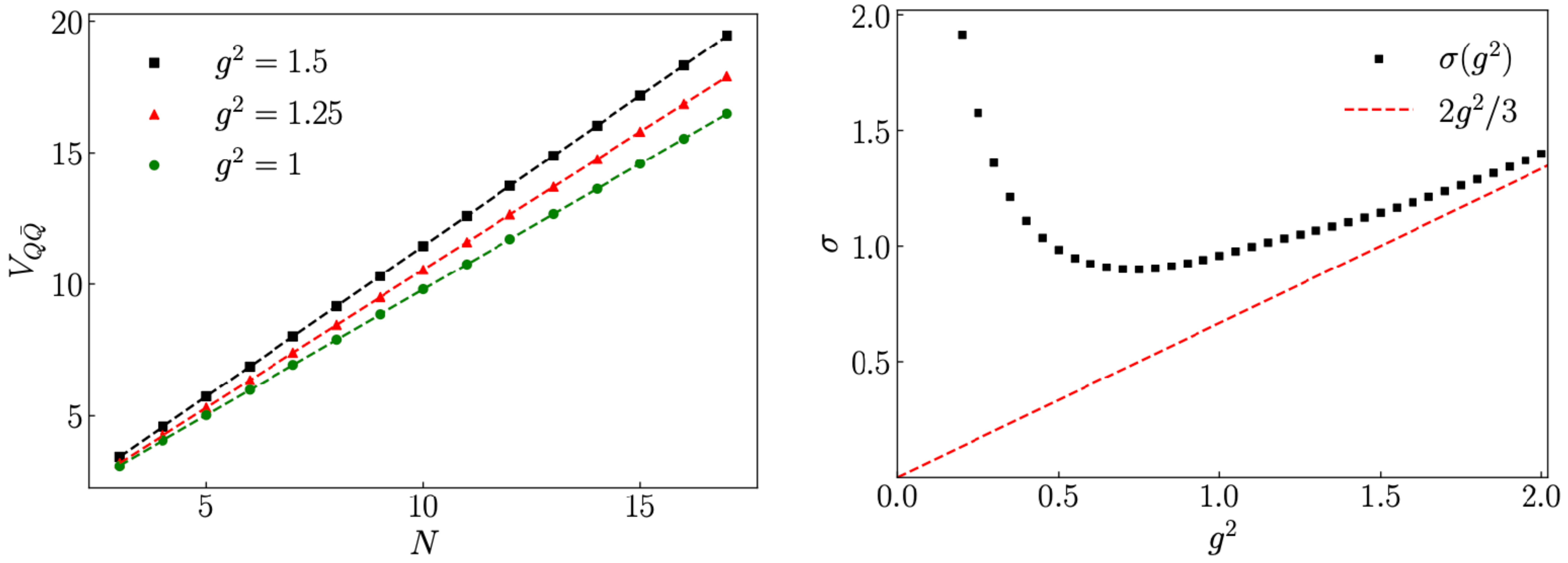

# String "melting"

$V_{Q\overline{Q}}$ drops rapidly with excitation energy (or micro canonical temperature) for excited states.

For high temperatures the potential becomes independent of $Q\overline{Q}$ distance!

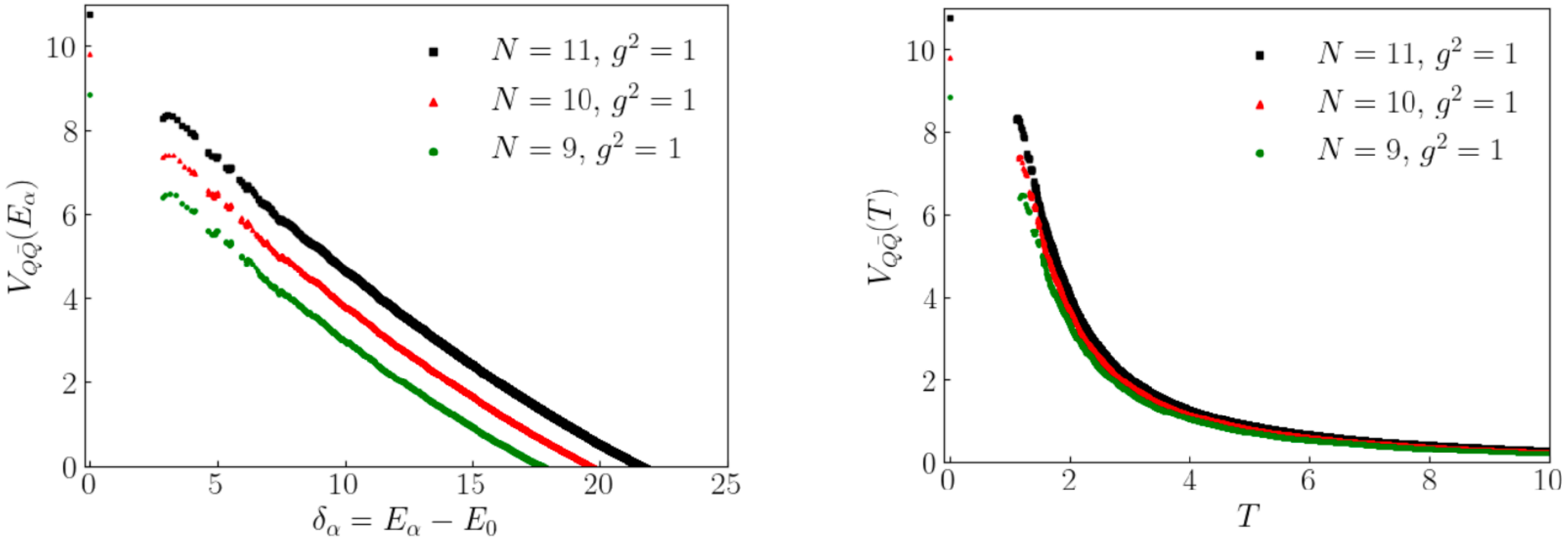

# $V_{Q\bar{Q}}$ versus $V_{QQQ}$

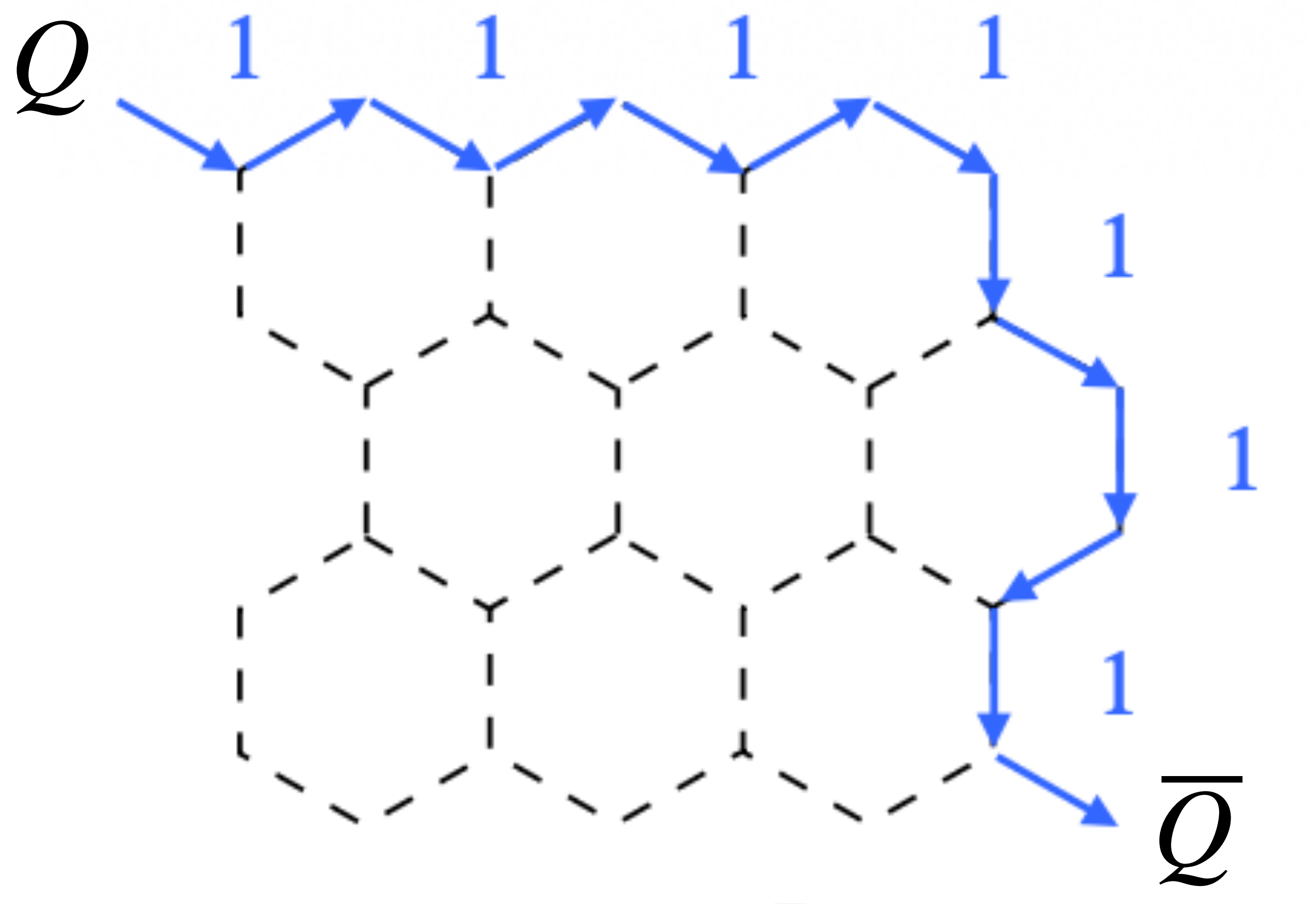


(a) $Q\bar{Q}$.

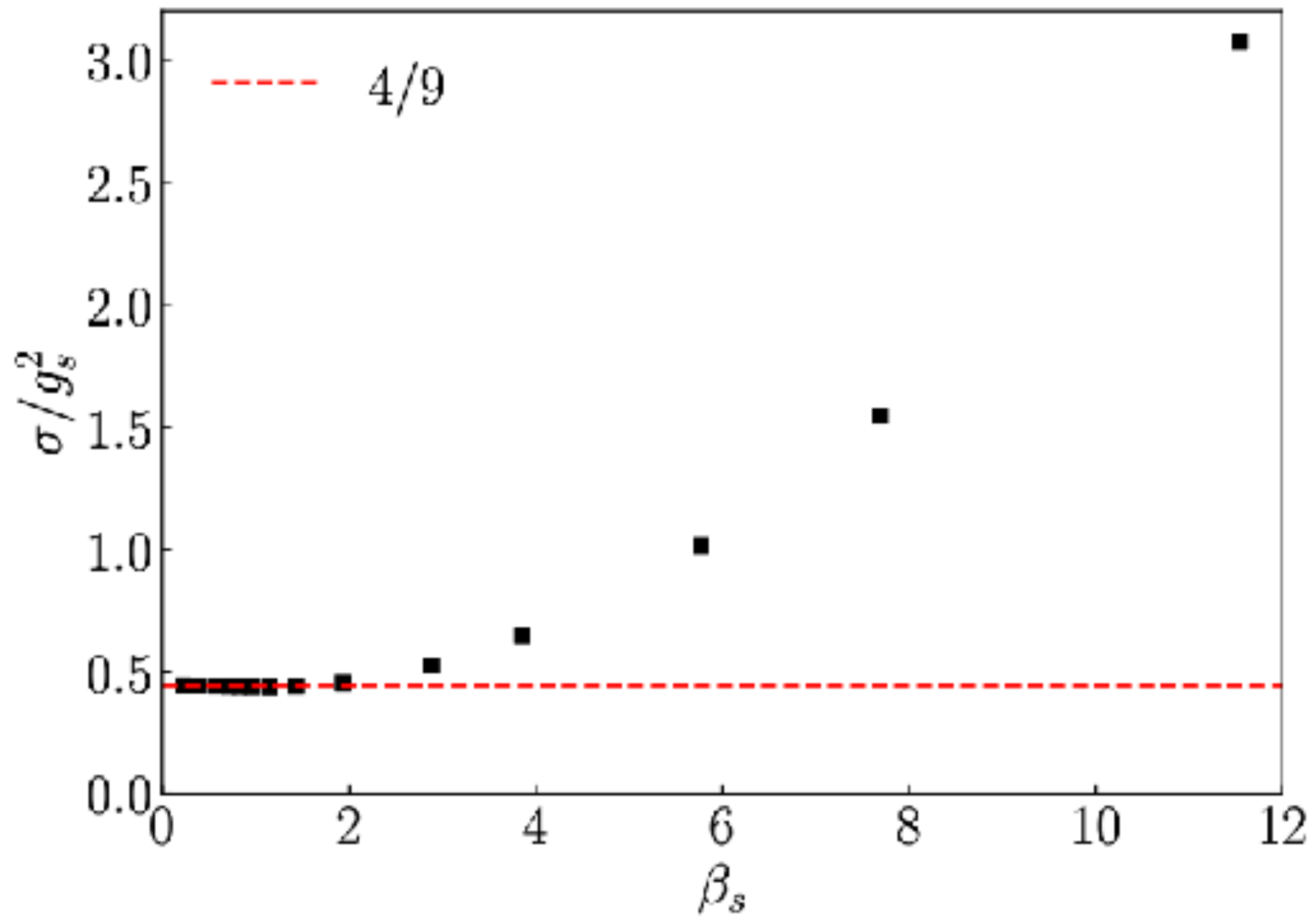


Coupling constant dependence of the $Q\bar{Q}$ string tension on the honeycomb lattice.

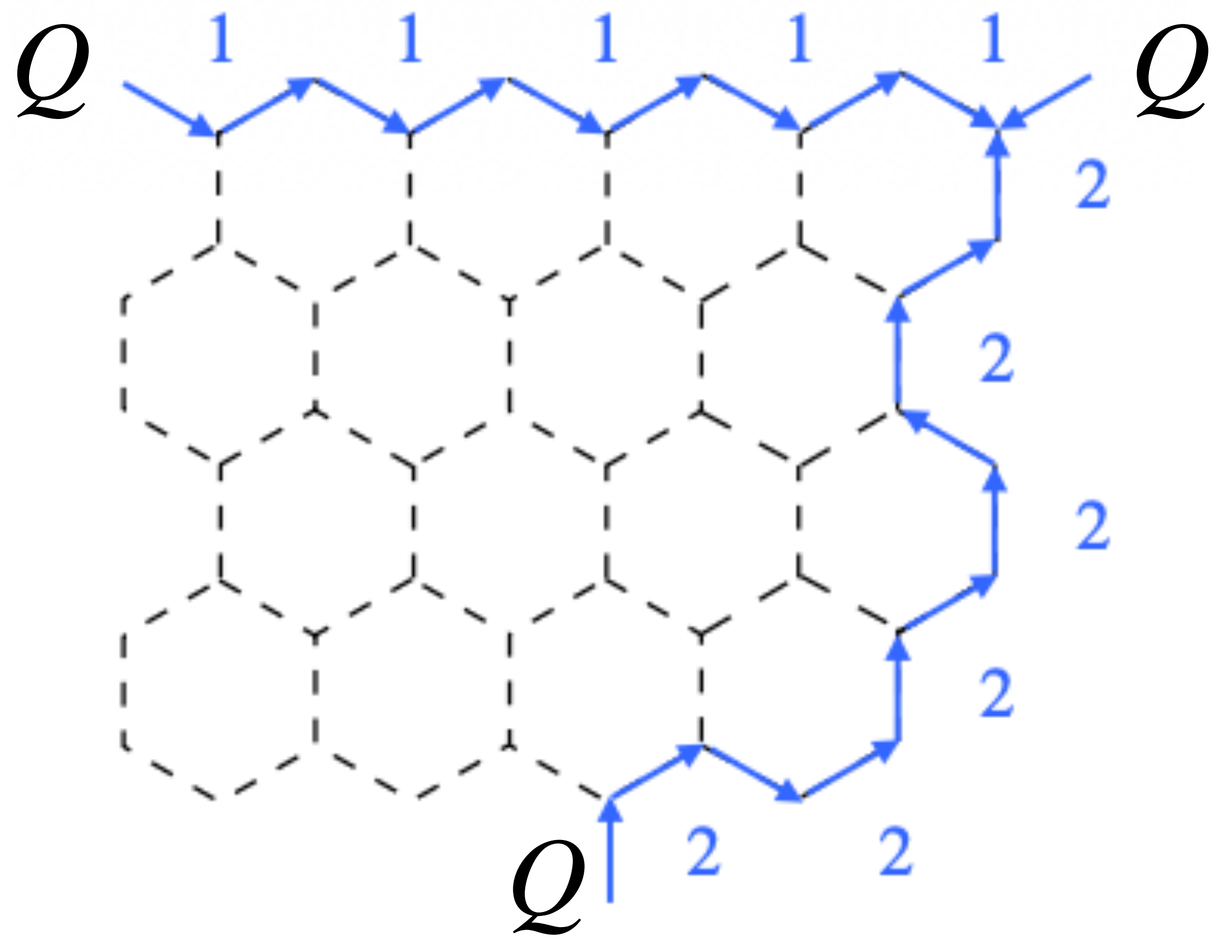


(b) $QQQ$.

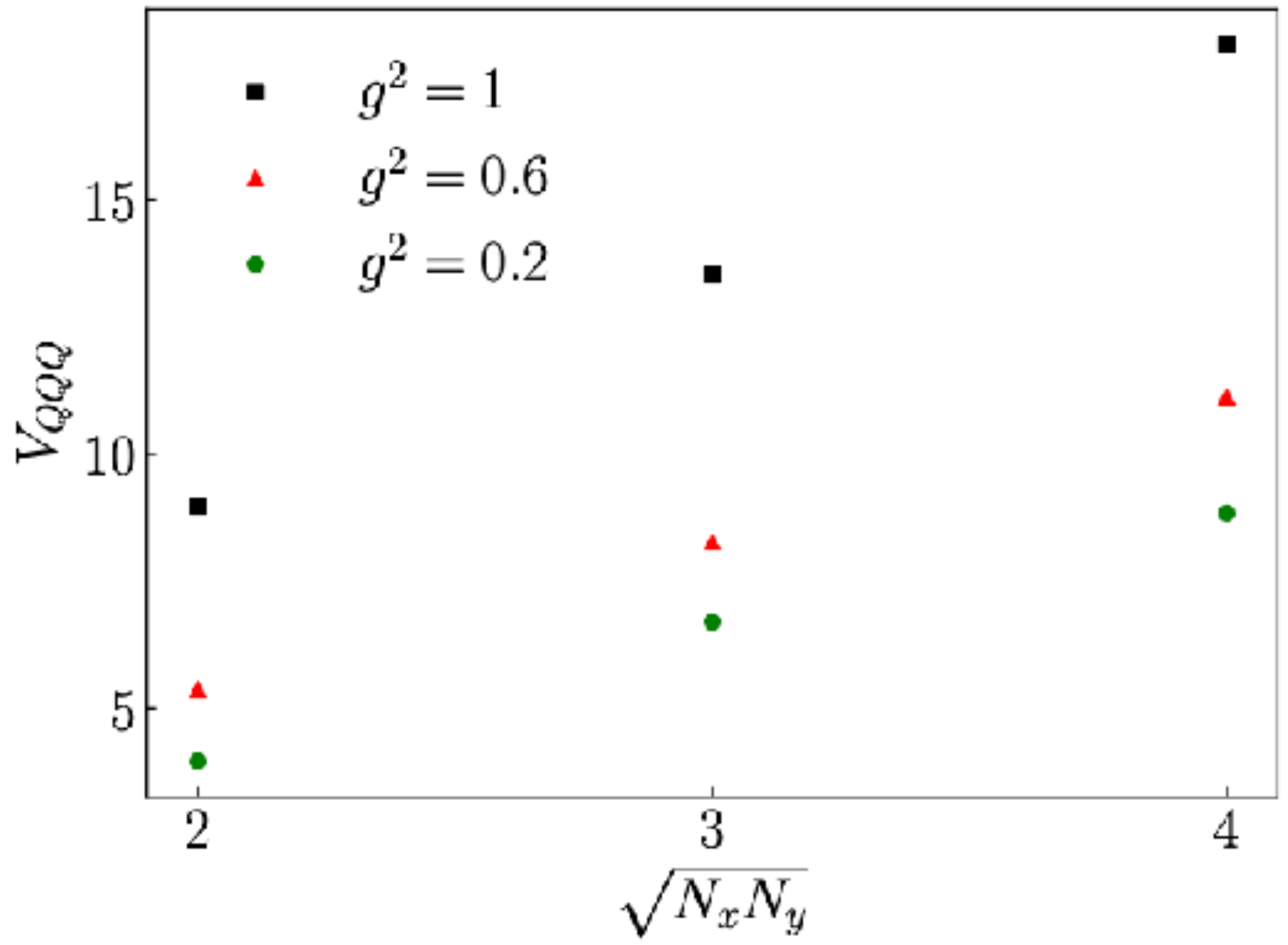


Confining potential for $QQQ$

# Summary

- First studies of thermalization behavior on small SU(2) lattices are encouraging
- Evidence for two-step thermalization for local observables
- In process: Thermalization on IBM quantum computer; glasma formation

- First results for SU(3) gauge theory on small lattices in the minimal truncation
- Strong evidence for quantum chaos
- First studies of confining $Q\overline{Q}$ and $QQQ$ potentials and string melting
- Future plans: Higher SU(3) representations; tensor networks; quantum computation
- 3-D lattices still look very hard; will require different QC architectures and better error correction at hardware level